

# Absence of a dissipative quantum phase transition in Josephson junctions: Theory

Carles Altimiras,<sup>1</sup> Daniel Esteve,<sup>1</sup> Çağlar Girit,<sup>1</sup> H el ene le Sueur,<sup>1</sup> and Philippe Joyez<sup>1,\*</sup>

<sup>1</sup>*Universit e Paris-Saclay, CEA, CNRS, SPEC  
91191 Gif-sur-Yvette Cedex, France*

(Dated: Date: January 15, 2025)

We investigate the resistively shunted Josephson junction (RSJ) at equilibrium, using linear response, an exact path integral technique and symmetry considerations. All three approaches independently lead to conclude that the superconducting-insulating quantum phase transition long believed to occur in the RSJ, cannot exist. For all parameters, we find that shunting a junction makes it more superconducting. We reveal that the UV cutoff of the resistor plays an unforeseen key role in these systems, and show that the erroneous prediction of an insulating state resulted in part from assuming it would not. We also explain why the RSJ physics differs from that of 1D quantum impurity problems. Our results fully support and confirm the experimental invalidation of this quantum phase transition by Murani *et al.* in 2020.

## I. INTRODUCTION

In the early 1980s Caldeira and Leggett [1] introduced a Hamiltonian allowing a rigorous quantum-mechanical description of arbitrary linear circuits connected to a Josephson junction (JJ). Using this Hamiltonian, they predicted quantitatively how dissipation reduces quantum tunneling of the junction’s phase –a macroscopic electrical variable– and it was precisely confirmed experimentally a few years later [2].

Shortly after Caldeira and Leggett introduced their modeling of dissipative systems, Schmid [3] predicted that a dissipative quantum phase transition (QPT) should occur for a quantum particle in a 1D periodic potential submitted to friction : Above a well-defined threshold in the friction strength, independent of the potential depth and particle mass, the particle localizes in one well of the potential, while below this threshold it is delocalized, in apparent continuity with the Bloch states that exist in absence of friction.

At the end of his Letter [3], Schmid briefly mentions a resistively shunted Josephson junction (RSJ) is analogous to the system he considers and suggests one could use it as a test bed to observe his predicted *localization* effect. In this analogy, the phase of the junction plays the role of the particle’s position, the friction strength scales as  $R^{-1}$ , the inverse of the shunt resistance, and Schmid’s analogy implies the junction’s phase should be localized only when the shunt resistance  $R$  is smaller than  $R_Q = h/4e^2 \simeq 6.5\text{k}\Omega$  and delocalized when  $R > R_Q$ , irrespective of the junction’s characteristics (size, transparency, material...). The standard interpretation of this localization|delocalization dissipative QPT is that, at  $T = 0$ , the JJ should be superconducting for resistances  $R < R_Q$  and *insulating* for  $R > R_Q$ . Even though this predicted insulating phase strangely conflicts with the perturbative limit  $R \rightarrow \infty$  and the classical understanding of JJs (see Appendix A), theoretical papers that examined the subject using many different techniques have, to the best of our knowledge, all essentially confirmed this interpretation [4–15] and the phenomenon was linked with quantum impurity problems [16, 17].

In 2020 Murani *et al.* [18] (including most of the present authors) used state-of-the-art experimental techniques to investigate SQUIDS, *i.e.* flux-tunable JJs, shunted with resistances  $R \geq 1.2R_Q$ . They observed a dc magnetic flux modulated the linear response (implying the SQUID loop hosted a dc supercurrent, hence not being insulating), but saw no trace of  $T$ -power-law dependence of this linear response at low temperatures, the expected hallmark of a quantum critical behavior [19]. Based on these experimental observations, Murani *et al.* concluded to the absence of the insulating state predicted by the standard interpretation of Schmid’s analogy for Josephson junctions. Subsequently, a number of papers [20–27] explicitly reaffirmed the existence of Schmid’s “insulating state” in Josephson junctions, at least in some parameter domain. Thus, the scientific community has not yet attained a consensus regarding the presence or absence of Schmid’s QPT in JJs. This underscores the current lack of a comprehensive theoretical understanding of the RSJ.

In this work, we bring full theoretical support to the conclusion of Murani *et al.* that RSJs are always superconducting in their ground state. To do so, we model the RSJ using the standard the Caldeira-Leggett Hamiltonian. By first applying Kubo’s linear response theory, we indeed simply prove that, at equilibrium, the junction is superconducting

---

\* *Misc:* philippe.joyez@cea.fr

for all parameters. Then, independently, we use an exact method based on the path integral formalism, from which we can predict the junction's state and transport properties. Already at the qualitative level of the path integral equations, we can rule out the existence of the predicted QPT, and we relate this to a ground state degeneracy of that model Hamiltonian that was not previously appreciated. Our numerical results show that, for all parameters tested, a resistively shunted Josephson junction is always more superconducting than the same unshunted junction. By highlighting differences between works predicting the QPT on one side and our present work and experiments on the other side, we elucidate how they came to predict a quantum phase transition.

## II. FORMULATION OF THE PROBLEM

We model the effect of dissipation on a Josephson junction in the same way as Caldeira and Leggett (CL) [1], with a bath of LC harmonic oscillators providing a linear viscous damping force proportional to the voltage across the junction (*i.e.* the time derivative of the junction's phase), independently of the value of the phase (See Fig. 1). The corresponding RSJ Hamiltonian is

$$H_0 = E_C N^2 - E_J \cos \varphi + \sum_n 4e^2 \frac{N_n^2}{2C_n} + \varphi_0^2 \frac{(\varphi_n - \varphi)^2}{2L_n}, \quad (1)$$

where  $\varphi_0 = \hbar/2e$  is the reduced flux quantum,  $\varphi$  (resp.  $N$ ) denotes the junction's phase (resp. number of Cooper pairs on the capacitor) which verify  $[\varphi, N] = i$ , and the  $\varphi_n$  (resp.  $N_n$ ) denote the phase (resp. dimensionless charge) of the bath harmonic oscillators.

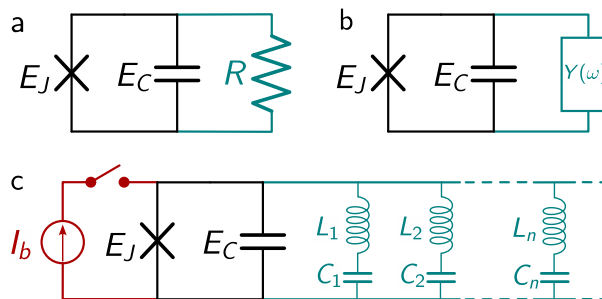


Figure 1. Various schematics of a RSJ. All panels : in black, the junction (cross symbol) and its intrinsic capacitance, forming together a Cooper pair box. In blue, a dissipative element shunting the junction. **a**: the dissipative element is generally depicted as a resistor **b**: A resistor always has a high frequency cutoff. Correspondingly, the complete frequency-dependent behavior is modeled here by an admittance  $Y(\omega)$ . **c**: In the Caldeira-Leggett Hamiltonian, the admittance is decomposed as shown : an infinite ensemble of  $LC$  resonators at all frequencies. For figuring the linear response of the RSJ, we may connect a current source as depicted in red.

The voltage operator across the parallel elements is  $V = \frac{2e}{C} N$  and the operator for the current in the junction is  $I_J = I_0 \sin \varphi$ , with  $I_0 = E_J/\varphi_0$ . The Hamiltonian (1) yields the equations of motion

$$V = \varphi_0 \dot{\varphi} \quad (2)$$

$$I_J = -2e \left( \dot{N} + \sum_n \dot{N}_n \right), \quad (3)$$

$$\dot{I}_J = \frac{E_J}{2\varphi_0^2} (\cos \varphi V + V \cos \varphi). \quad (4)$$

The first line is just the Josephson relation, the second line expresses current conservation, and the third line evidences an inductive character of the junction ( $\dot{I}_J \propto V$ ), at the operator level.

### A. Kubo linear response of the RSJ

We first use Kubo's linear response theory [28] to evaluate the transport properties of the system at equilibrium. Thus, we consider perturbing  $H_0$  by adding a small current-bias term  $-\varphi_0 \varphi I_b(t)$ , and seek the response expectation

value  $\mathcal{V}(t)$  (respectively,  $\mathcal{I}_J(t)$ ) of the voltage across the RSJ (resp., the current flowing in the junction) at first order in the perturbation. A straightforward application of Ref. [28] gives

$$\mathcal{V}(t) = \int_{-\infty}^{+\infty} z(t-t')I_b(t')dt' \ ; \ \mathcal{I}_J(t) = \int_{-\infty}^{+\infty} \chi(t-t')I_b(t')dt'$$

with the impulse response functions

$$\begin{aligned} z(t) &= -\frac{i}{\hbar}\theta(t)\langle[\varphi_0\varphi, V(t)]\rangle = -i\frac{R_Q}{2\pi}\theta(t)\langle[\varphi, \dot{\varphi}(t)]\rangle, \\ \chi(t) &= -\frac{i}{\hbar}\theta(t)\langle[\varphi_0\varphi, I_J(t)]\rangle = i\theta(t)\langle[\varphi, \dot{N}(t)]\rangle. \end{aligned} \quad (5)$$

In the above expressions,  $\mathcal{V}(t) = \text{Tr}(\Delta\rho(t)V)$  and  $\mathcal{I}_J(t) = \text{Tr}(\Delta\rho(t)I_J)$ , with  $\Delta\rho(t)$  the change of the density matrix at lowest order in  $I_b(t)$ ,  $\langle\bullet\rangle = \text{Tr}(\rho_{\text{eq}}\bullet)$  with  $\rho_{\text{eq}}$  the unperturbed density matrix and  $\bullet$  a generic placeholder,  $\theta(t)$  is the Heaviside step, and operators (except  $\Delta\rho(t)$ ) are evolved in the interaction picture  $\bullet(t) = e^{iH_0t/\hbar}\bullet e^{-iH_0t/\hbar}$ . For obtaining the final writing of  $z(t)$  and  $\chi(t)$ , we made use of the equations of motion (2-3), suited in this interaction picture, and of  $[\varphi, N_n] = 0$ .

In the following, we specifically consider a current step  $I_b(t) = \theta(t)I_b$ , for which we can rewrite

$$\begin{aligned} \mathcal{I}_J(t > 0) &= iI_b \int_0^t d\tau \langle[\varphi, \dot{N}(\tau)]\rangle \\ &= I_b(1 + i\langle[\varphi, N(t)]\rangle). \end{aligned}$$

In the second line, we performed the integration, and used  $[\varphi, N] = i$ . We now evaluate the dc value  $\overline{\mathcal{I}_J}$  of the above result as  $\overline{\bullet} = \lim_{T \rightarrow \infty} \frac{1}{T} \int_{t>0}^{t+T} d\tau \bullet(\tau)$ , yielding

$$\begin{aligned} \overline{\mathcal{I}_J} &= I_b(1 + i\langle[\varphi, \overline{N}]\rangle) \\ &= I_b, \end{aligned} \quad (6)$$

where  $\overline{N}$  it thus the time-invariant part of  $N(t)$ , which, consequently, commutes with  $H_0$  and  $\rho_{\text{eq}}$ . In the last step, we used  $\langle[\varphi, \overline{N}]\rangle = \text{Tr} \rho_{\text{eq}}[\varphi, \overline{N}] = \text{Tr}[\overline{N}, \rho_{\text{eq}}]\varphi = 0$ . Hence, at long times, at lowest order in  $I_b$ , the source's current entirely flows through the junction. Current conservation implies that no dc current flows through the resistor and Ohm's law then dictates that no dc voltage develops across the elements; the dc impedance  $\overline{\mathcal{V}}/I_b = 0$  is zero.

Still for this step current bias, from the above equations, we work out the derivatives at  $t = 0^+$  :

$$\begin{aligned} \frac{d\mathcal{V}}{dt}(t=0) &= -\frac{i}{\hbar}I_b\langle[\varphi_0\varphi, V]\rangle \\ &= \frac{I_b}{C} \end{aligned}$$

and, using (4),

$$\begin{aligned} \frac{d^2\mathcal{I}_J}{dt^2}(t=0) &= -\frac{i}{\hbar}\varphi_0 I_b \langle[\varphi, \dot{I}_J]\rangle \\ &= \frac{E_J}{\varphi_0^2} \frac{I_b}{C} \langle\cos\varphi\rangle \\ &= \frac{E_J}{\varphi_0^2} \langle\cos\varphi\rangle \frac{d\mathcal{V}}{dt}(0) \end{aligned} \quad (7)$$

which confirms that the junction is inductive, with, at equilibrium, an effective linear inductance

$$L_{\text{eff}} = \varphi_0^2/E_J \langle\cos\varphi\rangle, \quad (7)$$

as already derived in Ref. [18]. The above long-time dc superconducting response is due to this inductive behavior.

Thus, Kubo's approach yields a superconducting dc linear response for all parameters of this Hamiltonian, and, remarkably, this result is independent of most system details. It does not depend on the actual presence of the dissipative bath, and applies for any lumped circuit where a generalized inductive element (*i.e.* with a phase-dependent energy) is in parallel with a capacitor (even an intrinsic or a parasitic one), *e.g.* a Cooper pair box, a weak link, a

parallel RLC circuit,... As well, the dc result (6) depends only on operator relations, not on the system's equilibrium *state*. Thus, were a QPT to occur in that system, it would not manifest as a superconducting-to-insulating transition. Later in this article we show with other arguments that, moreover, the localization|delocalization QPT predicted by Schmid does not occur in this model of the RSJ.

The above Kubo linear response is often considered in the frequency domain. Taking the Fourier transform of (5) and making use of the detailed balance, one obtains a form of the fluctuation-dissipation theorem

$$\text{Re } Z(\omega) = \frac{R_Q}{4\pi} (1 - e^{-\beta\hbar\omega}) \omega S_{\varphi\varphi}(\omega)$$

where  $Z(\omega) = \int z(t) e^{i\omega t} dt$  is the zero-bias linear impedance of the RSJ as seen from the current source, and  $S_{\varphi\varphi}(\omega)$  is the spectral density of phase fluctuations, *i.e.* the Fourier transform of the correlator  $\langle \varphi(t)\varphi \rangle$ . Schmid [3], Schön and Zaikin [9], and many other authors, determine the insulating or superconducting character of the junction by evaluating the so-called *dc mobility*  $\lim_{\omega \rightarrow 0} (\omega S_{\varphi\varphi}(\omega))$ . This quantity is indeed proportional to  $\text{Re } Z(\omega = 0) = \bar{V}/I_b$ , provided one ensures  $\hbar\omega \gg kT$  while taking the limit. Clearly, the non-zero dc mobility for  $R > R_Q$  predicted by Schmid [3] and confirmed countless times in the literature, is inconsistent with the null result obtained above in the time-domain. Later, we explain what could lead to finding a transition to a non-zero value of the mobility.

## B. Detailed description of the RSJ

In order to actually provide dissipation, the bath oscillators in (1) are in infinite number, forming a continuum in the frequency domain, characterized by the spectral density of modes

$$J(\omega) = \frac{\pi}{2} \sum_{n=1}^N \omega_n^2 Y_n \delta(\omega - \omega_n) = \omega \text{Re} Y(\omega),$$

where  $\omega_n = 1/\sqrt{L_n C_n}$  is the  $n^{\text{th}}$  mode angular frequency,  $Y_n = \sqrt{C_n/L_n}$  its admittance, and  $Y(\omega)$  the admittance formed by the continuum. Although this model and the numerical technique we employ below can handle any form of the admittance, we will focus here on the so-called Ohmic case where  $\text{Re} Y(\omega = 0) = 1/R$ , with  $R$  the dc shunting resistance, such that  $J(\omega)$  is linear in frequency at low frequency. For fundamental reasons, any concrete dissipative bath has a UV cutoff frequency [1]. Here, we assume that  $\text{Re} Y(\omega)$  has a Lorentzian shape

$$\text{Re} Y(\omega) = \frac{R^{-1}}{1 + (\omega/\omega_c)^2} \quad (8)$$

which would correspond to a  $LR$  series circuit, with  $\omega_c = R/L$ . In a practical implementation of a metallic resistor, the inductance  $L$  would be at least the geometrical inductance of the device. Quantitative predictions on the system will depend on the precise shape of the cutoff, but, when only qualitative understanding is sought, it may be simpler to reason with other cutoff shapes (e.g. abrupt or exponential). In any case, our modeling enables considering the theoretical  $\omega_c \rightarrow \infty$  limit.

The quadratic forms where the junction's phase appears in the last term of (1) can be expanded, giving

$$H_0 = H_{\text{CPB}} + H_{\text{bath}} + H_{\text{coupling}} + H_{\text{CT}}$$

with the different parts corresponding, respectively, to a bare Cooper pair box (CPB)

$$H_{\text{CPB}} = E_C N^2 - E_J \cos \varphi, \quad (9)$$

the uncoupled bath of harmonic oscillators

$$H_{\text{bath}} = \sum_n \frac{(2eN_n)^2}{2C_n} + \frac{(\varphi_0 \varphi_n)^2}{2L_n} = \sum_n \hbar\omega_n \left( a_n^+ a_n + \frac{1}{2} \right),$$

the coupling term

$$H_{\text{coupling}} = -\varphi_0 \varphi \times \left( \sum_n \varphi_0 \frac{\varphi_n}{L_n} \right) = -\varphi_0 \varphi \times I_Y$$

where the junction phase  $\varphi$  couples to the current  $I_Y$  flowing in the admittance  $Y(\omega)$ , and the so-called counter-term

$$\begin{aligned} H_{\text{CT}} &= (\varphi_0\varphi)^2 \sum_n \frac{1}{2L_n} \\ &= (\varphi_0\varphi)^2 \int_0^\infty \frac{d\omega}{\pi} \text{Re}Y(\omega) = \frac{(\varphi_0\varphi)^2}{2L} \\ &= E_L\varphi^2, \end{aligned}$$

which appears as a parabolic inductive potential term for the junction phase and which is essential for having the expected damped equations of motion in the classical limit [1]. Interestingly, the counter-term transforms our CPB Hamiltonian into a fluxonium [29] Hamiltonian at zero external flux

$$H_{\text{CPB}} + H_{\text{CT}} = H_{\text{F1}}.$$

At this point we highlight that the coupling term scales as  $1/R$ , making it perturbative in the large  $R$  limit. Note that if one considers a fixed cutoff frequency, the counter-term inductive energy  $E_L$  also vanishes as  $1/R$  (since  $1/L = \omega_c/R$ ). Thus, in this Caldeira-Leggett model, a very large shunt resistor appears as a perturbation to the CPB, in agreement with the intuitive expectation that when  $R$  increases to infinity no current can flow into it, so that dissipation disappears and one can just remove the resistance from the circuit. In the case of a purely inductive shunt with  $L \rightarrow \infty$ , one also recovers the physics of a CPB [30] (but we will not appeal to this result in the following).

### III. EQUILIBRIUM REDUCED DENSITY MATRIX FROM PATH INTEGRALS

The equilibrium reduced density matrix (RDM) of the CPB (i.e. the junction and its capacitor) at temperature  $T$  is obtained as

$$\rho_\beta = \frac{1}{Z} \text{Tr}_b e^{-\beta H}, \quad (10)$$

where  $\beta = (k_B T)^{-1}$  is the inverse temperature,  $Z = \text{Tr}[\exp(-\beta H)]$  is the partition function of the entire system, and  $\text{Tr}_b$  corresponds to tracing out the bath oscillators. For the linear coupling term and the harmonic bath we have, this tracing out can be performed exactly, yielding the matrix elements of the RDM in phase representation as a path integral in imaginary time [1, 31–33]

$$\rho_\beta[\phi, \phi'] = \frac{1}{Z} \int \mathcal{D}\varphi \exp \left[ -\frac{1}{\hbar} (S_{\text{F1}}^E[\varphi] + \Phi[\varphi]) \right], \quad (11)$$

where the functional integral is over all imaginary time paths  $\varphi(\tau)$  having the boundaries  $\varphi(0) = \phi$  and  $\varphi(\hbar\beta) = \phi'$ . In this expression, the terms in the exponential respectively denote the Euclidean action of the fluxonium

$$S_{\text{F1}}^E[\varphi] = \int_0^{\hbar\beta} d\tau \mathcal{L}_{\text{F1}}[\varphi], \quad (12)$$

with  $\mathcal{L}_{\text{F1}}[\varphi] = \frac{\hbar^2}{4E_C} \dot{\varphi}^2 - E_J \cos \varphi + E_L \varphi^2$ , the Lagrangian of the fluxonium and

$$\Phi[\varphi] = -\frac{1}{2} \int_0^{\hbar\beta} d\tau \int_0^{\hbar\beta} d\tau' \varphi(\tau) K(\tau - \tau') \varphi(\tau'), \quad (13)$$

the Feynman-Vernon influence functional [31], with the kernel

$$K(\tau) = \frac{R_Q}{2\pi} \mathcal{C}_{II}(-i\tau) \quad (14)$$

where  $\mathcal{C}_{II}$  is the equilibrium autocorrelation function of the current in the admittance (shunted at its ends). For  $t \in \mathbb{R}$ ,  $\mathcal{C}_{II}(t)$  is obtained using the quantum fluctuation-dissipation theorem and the Wiener-Khinchin theorem

$$\mathcal{C}_{II}(t) = 2 \int_{-\infty}^{\infty} \hbar\omega \text{Re}Y(\omega) \frac{e^{-it\omega}}{(1 - e^{-\beta\hbar\omega})} \frac{d\omega}{2\pi} \quad (15)$$

which shows that without a UV cutoff in  $\text{Re}Y(\omega)$ ,  $\mathcal{C}_{II}(t)$  would be divergent for all  $t \in \mathbb{R}$  and hence nonphysical. In Eq. (14) this expression is simply prolonged to complex times, yielding

$$K(\tau) = \frac{R_Q}{2\pi} \int_0^{+\infty} \hbar\omega \text{Re}Y(\omega) \frac{2 \cosh \left[ \left( \frac{\beta\hbar}{2} - \tau \right) \omega \right] d\omega}{\sinh \frac{\beta\hbar\omega}{2}} \frac{1}{2\pi}, \quad (16)$$

and one can check that  $\int_0^{\beta\hbar} d\tau K(\tau) = 2E_L$ . In Appendix B, we provide analytical expressions for  $K(\tau)$ , for the Lorentzian  $\text{Re}Y(\omega)$  we consider. In Appendix D 1, we show that our action is consistent with that used by Schmid and other authors, although we have a more general kernel in the influence functional.

### A. Hubbard-Stratonovich transformation

For evaluating the path integral (11), we then rewrite the influence functional by means of a Hubbard-Stratonovich [34, 35] transformation. In this process, one introduces an auxiliary random scalar field  $\xi(\tau)$  having Gaussian fluctuations verifying

$$\langle \xi(\tau)\xi(\tau') \rangle = \mathcal{C}_{II}(-i(\tau - \tau')), \quad (17)$$

such that the double integral in Eq. (13) involving  $\varphi$  at two different imaginary times can be replaced by a single integral involving  $\varphi$  at only one time, averaged over all possible realizations of  $\xi$  [36–38]. Upon this exact transformation, Eq. (11) becomes :

$$\rho_\beta[\phi, \phi'] = \frac{1}{Z} \int \mathcal{D}\xi W[\xi] \int \mathcal{D}\varphi \exp \left[ -S_{\text{FI}}^E[\varphi] - \frac{1}{\hbar} \int_0^{\hbar\beta} d\tau \xi(\tau) \varphi_0 \varphi \right],$$

with a Gaussian weight functional  $W[\xi]$  ensuring Eq.(17). In the last expression, the terms in the exponential can be seen as the Euclidean action of a fictitious system made of a fluxonium coupled to a given realization of a random “current noise”  $\xi(\tau)$  generated by the bath, so that Eq. (11) is now reformulated as

$$\rho_\beta[\phi, \phi'] = \frac{1}{Z} \int \mathcal{D}\xi W[\xi] \int \mathcal{D}\varphi \exp \left[ -\frac{1}{\hbar} S_{\text{Fict}}^E[\varphi, \xi] \right], \quad (18)$$

with

$$S_{\text{Fict}}^E[\varphi, \xi] = \int_0^{\hbar\beta} d\tau \left( \frac{\hbar^2}{4E_C} \dot{\varphi}^2 - E_J \cos \varphi + E_L \varphi^2 + \xi \varphi_0 \varphi \right). \quad (19)$$

#### 1. Invalidation of Schmid’s QPT

At this point, one can realize that valid states for these equations all have a finite extent in  $\varphi$ . Indeed, in the action of Eq. (19), when  $0 < E_L = \hbar\omega_c R_Q/4\pi R$ , the counter-term  $E_L \varphi^2$  acts as a confining potential since it dominates other terms at large  $|\varphi|$  (the random noise  $\xi$  is  $\varphi$ -independent, and Gaussian-distributed with a finite variance  $\mathcal{C}_0$  for its mean value given by (B2)). Hence, as long as  $\omega_c > 0$  and  $R < \infty$ , the ground state of the action (18-19) is localized for all parameters. Given the link between Schmid’s action and ours (see Appendix D 1), the localized ground state yielded by our equations is also a valid ground state for his action, for any  $R < \infty$ . This rules out the ground state localization|delocalization transition Schmid predicts at  $R = R_Q$ .

The always-localized states we obtain may seem to break the discrete translational symmetry present in the Caldeira-Leggett Hamiltonian (1) and to be in conflict with the intuitive understanding of Schmid’s prediction presented in the Introduction that, at weak damping, the states of the system should resemble the Bloch states that exist in absence of damping. In Appendix E, we show that there is actually no problem there: the translational symmetry of the Hamiltonian makes the states infinitely degenerate in that system, such that, for  $R < \infty$ , one can exhibit infinitely many ground states, either localized (like ours) or non-dispersing Bloch-like delocalized with respect to the junction’s phase. However, since the junction’s phase is not measurable, all these ground states are indiscernible, which makes discussing about a localization|delocalization QPT futile.

In the following we show that our path integral approach enables for the first time to make quantitative numerical predictions for the RSJ. We illustrate this for various parameters, with some qualitative understanding of the observed variations. In the process, we can explain why previous authors came to predict a QPT.

## B. Stochastic Liouville equations

For any given realization of  $\xi(\tau)$  in Eq. (18), the integral of the action of the fictitious system over all  $\varphi$  paths can be seen as an element  $\rho_\xi[\phi, \phi']$  of a (non-normalized) RDM obeying the imaginary-time stochastic Liouville equation

$$-\hbar \frac{\partial}{\partial \tau} \rho_\xi = (H_{\text{FI}} + \xi(\tau) \varphi_0 \varphi) \rho_\xi \quad (20)$$

of the fictitious fluxonium coupled to the noise source  $\xi(\tau)$ , so that (18) reads

$$\rho_\beta[\phi, \phi'] = \frac{1}{Z} \int \mathcal{D}\xi W[\xi] \rho_\xi[\phi, \phi'].$$

The later equation translates into a path integral equation for the RDM operators, independently of any choice of basis

$$\rho_\beta = \frac{1}{Z} \int \mathcal{D}\xi W[\xi] \rho_\xi. \quad (21)$$

For obtaining the physical equilibrium RDM of the CPB one then needs to perform the remaining path integral over  $\xi$  in Eq. (21). This can be done using the following scheme. For a given realization of  $\xi(\tau)$ , one starts with  $\rho_\xi(\tau = 0)$  an equipartitioned diagonal matrix (corresponding to an infinite temperature state of the fictitious fluxonium, appropriate for  $\tau = 0$ ) and integrates (20) up to  $\rho_\xi(\tau = \hbar\beta)$ . This yields a non-normalized RDM matrix with no particular physical meaning. Repeating this numerical integration for a suitable number of drawings of the random noise obeying Eq. (17) amounts to sampling  $W[\xi]$ , and the normalized average of the different  $\rho_\xi(\hbar\beta)$  is expected to converge to the physical equilibrium RDM

$$\frac{\sum \rho_\xi(\hbar\beta)}{\text{Tr} \sum \rho_\xi(\hbar\beta)} \rightarrow \rho_\beta.$$

We stress that if this stochastic averaging converges properly, the resulting density matrix is exact; it takes into account the interaction of the system and the bath to all orders with no approximation. Let us also note that the above path integral method can be applied to any open system at equilibrium where position-like degrees of freedom are linearly coupled to a linear bath. It can be extended to cases where the system-bath coupling is a non-linear function of the system's coordinates [38]. It can even be extended to real-time out-of-equilibrium dynamics of the system [36, 38] at the price of introducing additional complex cross-correlated real-time stochastic variables.

### 1. Numerical implementation

For the numerical implementation of the above stochastic method, we choose as working basis the  $\mathcal{K}$  lowest eigenstates  $\{|\Psi_k\rangle, 0 \leq k \leq \mathcal{K} - 1\}$  of the uncoupled fluxonium (the expected finite extent of the ground state in  $\varphi$  ensures that such truncation is possible). For obtaining these eigenstates, we use an intermediate discretized phase basis  $\{\varphi_j = j\delta\varphi, \delta\varphi \ll 2\pi, j \in \mathbb{Z}, |j| < \varphi_{\text{max}}/\delta\varphi\}$ , with  $N^2 = -\partial^2/\partial\varphi^2$  approximated as a finite difference, so that the Hamiltonian is a tridiagonal matrix in this discretized phase basis. Optimized diagonalization routines yield the first a few hundred eigenstates of such tridiagonal matrices very fast, even when  $\pm\varphi_{\text{max}}$  spans many wells of the cosine (low  $E_L$ ).

Note that our working basis is *very* different from that of the bare CPB which is the reference system we are interested in; this fluxonium basis has notably a much greater density of levels [30]. At low temperature, the most relevant energy scale for the bare CPB is its transition energy from the ground state to the first excited state  $\hbar\omega_{01} = E_1 - E_0$  at zero offset charge (see Appendix C), which varies from  $\hbar\omega_{01} \simeq E_C$  when  $E_C \gg E_J$  to  $\hbar\omega_{01} \simeq \sqrt{E_J E_C}$  in the opposite limit  $E_J \gg E_C$ . This is the ‘‘natural’’ energy scale we consider in the following, not the transition frequencies of the fluxonium. We choose the truncation of the working basis to encompass all the energy scales we take into account (and  $\varphi_{\text{max}}$  in the intermediate basis is set accordingly).

Then, in the working basis, the stochastic differential Liouville equation (20) is numerically integrated using discrete imaginary times steps  $\{\tau_m = m\delta\tau\}$ , with  $\delta\tau = \hbar\beta/M$  and  $0 \leq m \leq M - 1$ , and starting with  $\rho(\tau = 0) = I_{\mathcal{K}}/\mathcal{K}$ , with  $I_{\mathcal{K}}$  the identity matrix. The actual approximate integration of (20) is performed using the symmetric Trotter iteration scheme

$$\rho_\xi(\tau_{m+1}) = \exp\left(\varphi_0 \varphi \xi(\tau_m) \frac{\delta\tau}{2\hbar}\right) \cdot \exp\left(-H_{\text{FI}} \frac{\delta\tau}{\hbar}\right) \cdot \exp\left(\varphi_0 \varphi \xi(\tau_m) \frac{\delta\tau}{2\hbar}\right) \cdot \rho_\xi(\tau_m) \quad (22)$$

that preserves the positivity of the RDM at each step [39]. In Appendix B, we explain how we generate the random noises  $\xi(\tau_m)\delta\tau$  entering this iteration scheme.

As explained above, after numerically integrating Eq. (20) for  $P$  different realizations of  $\xi$ , we take the average RDM as

$$\bar{\rho} = \frac{\sum_{p=1}^P \rho_{\xi_p}(\hbar\beta)}{\text{Tr} \sum_{p=1}^P \rho_{\xi_p}(\hbar\beta)}. \quad (23)$$

In the large  $P$  limit, this averaged RDM is expected to tend to the true equilibrium RDM, which must be Hermitian and positive-semidefinite. After a finite number of drawings,  $\bar{\rho}$  is not perfectly Hermitian-symmetric, however, it is legitimate to symmetrize it. Indeed, for the problem we consider and in the basis we use, for a given drawing of the  $\{\xi(\tau_m)\}$  yielding  $\rho_\xi$ , drawing the reversed sequence  $\{\xi(\tau_{M-1-m})\}$  is equally probable and would yield the transposed of  $\rho_\xi$  (in our working basis, all the matrices in (22) are real). Hence, for each drawing we may just add  $\rho_\xi$  and its transposed matrix to our stochastic average, so that it always remain (Hermitian-) symmetric and positive-semidefinite (up to numerical accuracy). Note that even without such symmetrization, when the average converges properly (see below), the asymmetry of  $\bar{\rho}$  reduces as  $P$  increases, such that symmetrizing or not the RDM does not perceptibly change the expectation values of the observables we consider below.

While obtaining the RDM, we can simultaneously evaluate expectation values of any operator  $A$ , as

$$\langle A \rangle = \text{Tr} \bar{\rho} A = \frac{\sum w_p \text{Tr} \hat{\rho}_p A}{\sum w_p} = \frac{\sum w_p a_p}{\sum w_p}$$

where  $w_p = \text{Tr} \rho_{\xi_p}(\hbar\beta)$ ,  $\hat{\rho}_p = \rho_{\xi_p}(\hbar\beta)/w_p$  is the normalized RDM resulting from the integration of Eq. (20) with the  $p^{\text{th}}$  noise realization and  $a_p = \text{Tr} \hat{\rho}_p A$  the corresponding (nonphysical) expectation value of  $A$ . In this expression, the trace of the  $\rho_{\xi_p}(\hbar\beta)$  hence appear as the weight of a given noise realization in the final estimate of any expectation value (drawings with large traces correspond to paths with lower action in the path integral). The error bars on the estimated expectation value are obtained from the estimator of the variance of the weighted average using the Central Limit Theorem and the effective number of data points  $P_{\text{eff}}(P) = (\sum w_p)^2 / \sum w_p^2$ .

At large shunt resistance values and high temperature, the  $\{w_p\}$  are such that the effective number of samples  $P_{\text{eff}}(P)$  grows fast with the number of drawings  $P$  and the weighted means converge well. However, when reducing  $R$  (*i.e.* increasing the coupling to the bath) at fixed  $E_C, E_J, \hbar\omega_c$  and  $kT$ , one must increase the number of time steps needed to keep the random increments  $\xi(\tau_m)d\tau$  small enough, but after the random walk integration of Eq. (20) this nevertheless translates into an increased variance of the  $\{w_p\}$ , and a corresponding reduction of  $P_{\text{eff}}$ . At some point in this increase, the weighted estimation of the expectation values becomes dominated by the few drawings that fall in the (positive side) tail of the  $w_p$  distribution. In other words, when  $R$  is much reduced, the average is dominated by very few drawings (and possibly a single one when  $P_{\text{eff}} \simeq 1$  and no longer grows substantially with  $P$ ). This indicates that, in this case, the action has a deep and sharp minimum representing only an extremely small volume in the phase space of the  $\xi$  noise, making the method extremely inefficient. In such case, whether or not the method can still yield reliable estimates of observables depends on the derivatives of those observables around this minimum. Similarly, when reducing the temperature (all other parameters kept fixed), the number  $M$  of steps in  $\tau$  also needs to be scaled up, eventually causing the same poor statistics. The  $R$  and  $T$  ranges where the statistics are poor depend on the other system parameters, and notably on the cutoff frequency. The data presented below are all in regimes where the estimators have small error bars, away from these problematic limits.

#### IV. RESULTS

In Fig. 2 we show the expectation values of the rms charge fluctuations  $\sigma_N = \langle N^2 \rangle^{1/2}$  and the effective Josephson coupling ( $\cos \varphi$ ) as a function of the reduced temperature  $kT/\hbar\omega_{01}$ , for different values of  $E_J/E_C$ , for the RSJ at large values of  $R/R_Q$ . The finite values reached by these expectation values at low temperature attest that the junction allows (super)current flow in its ground state. Indeed, if the junction were insulating, its effective inductance  $L_{\text{eff}} = \varphi_0^2/E_J \langle \cos \varphi \rangle$  would be infinite (the Josephson coupling  $E_J \langle \cos \varphi \rangle$  vanishes) and the charge  $N$  on the capacitor would fluctuate just as in the  $C||Y$  circuit, yielding

$$\sigma_{N,C||Y} = \frac{C}{2e} \left( \int_{-\infty}^{\infty} \hbar\omega \text{Re} \frac{1}{iC\omega + Y(\omega)} \coth \left( \frac{\hbar\omega}{2kT} \right) \frac{d\omega}{2\pi} \right)^{1/2}.$$



For the Lorentzian admittance (8) we consider,  $C||Y$  is equivalent to a series RLC circuit, yielding the zero point fluctuations [1, 40]

$$\sigma_{N,C||Y}(T=0) = \left( \frac{\hbar\omega_c}{4\pi E_C} \frac{\log(\sqrt{\alpha} + \sqrt{\alpha-1})}{\sqrt{\alpha}\sqrt{\alpha-1}} \right)^{1/2}, \quad (24)$$

with  $\alpha = \frac{\pi R \hbar \omega_c}{4 R_Q E_C}$ . The conducting character of the JJ is evidenced by the fact that  $\sigma_N$  saturates to values strictly larger than  $\sigma_{N,C||Y}(T=0)$ , consistently with the finite saturation value of  $\langle \cos \varphi \rangle$ .

In that Fig. 2, we also compare our numerical results for these observables to those obtained for the thermal averages of the bare CPB considering all gate charge values (see Appendix C). For these large resistances, most of the numerical expectation values for the RSJ are found close to that of the CPB. At low temperatures they are found slightly above those of the CPB, but by increasing further the resistance (data not shown) one recovers more closely the bare CPB results, as expected for a vanishing perturbation. At large temperatures, some results for  $\sigma_N$  are slightly below the asymptote  $\sqrt{kT/2E_C}$  (valid for both the bare CPB and the  $C||Y$  circuit), which we attribute to our basis truncation.

In Fig. 3 we consider the  $R$ -dependence of the same expectation values for different ratios  $E_J/E_C$  and at the low temperature  $kT = 0.01\hbar\omega_{01}$ . We observe that both  $\langle \cos \varphi \rangle$  and  $\sigma_N$  smoothly increase when  $R$  is reduced. In Fig. 4, we show that for large resistance values, large  $E_C/E_J$  and at the low temperature  $kT = 0.005\hbar\omega_{01}$ , changing the cutoff frequency  $\omega_c$  of the environment admittance has a weak effect at small  $\omega_c$ , while at large  $\omega_c$ , the expectation values of the RSJ do depend on the actual value of the bath cutoff, the junction becoming more superconducting as  $\omega_c$  increases. Similar behavior is observed for other  $E_C/E_J$  ratios and shunt resistances values.

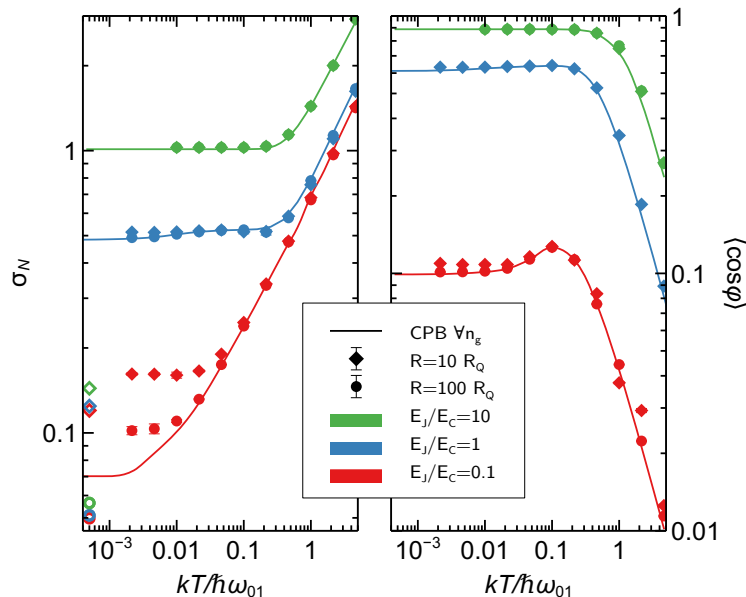


Figure 2. Temperature dependence of the rms charge fluctuations  $\sigma_N$  on the capacitor (left panel) and the Josephson coherence factor  $\langle \cos \varphi \rangle$  (right panel) for large shunt resistance values and different  $E_J/E_C$  ratios, for  $\hbar\omega_c = 0.4\hbar\omega_{01}$ . In both panels, the solid lines are the thermal expectation values for the unshunted CPB allowing any gate charge (See Appendix C). For larger resistance values, the calculated expectation values (markers) are getting closer to the bare CPB values, as expected for a vanishing perturbation. Open symbols in the left panel are the zero temperature limits of  $\sigma_{N,C||Y}$  (Eq. (24)) with the same  $Y(\omega)$  (same resistance and cutoff) as the filled symbol of corresponding color and shape. The fact that  $\sigma_N$  saturates above these values shows that the junction has finite supercurrent fluctuations in its ground state, consistent with the finite value of the Josephson coherence in the right panel.

Our method further allows to simply work out the dc linear response of the RSJ to a current bias. Indeed, adding a dc current source  $I_b$  to the system adds a potential term  $-\varphi_0 I_b \varphi$  to the Caldeira-Leggett Hamiltonian (1), and this term directly carries over to our path integrals, shifting the minimum of the potential of the fictitious fluxonium away from  $\varphi = 0$ . With this term added, for small bias current  $I_b \ll I_0 = E_J/\varphi_0$ , stochastic Liouville numerics (see Fig.

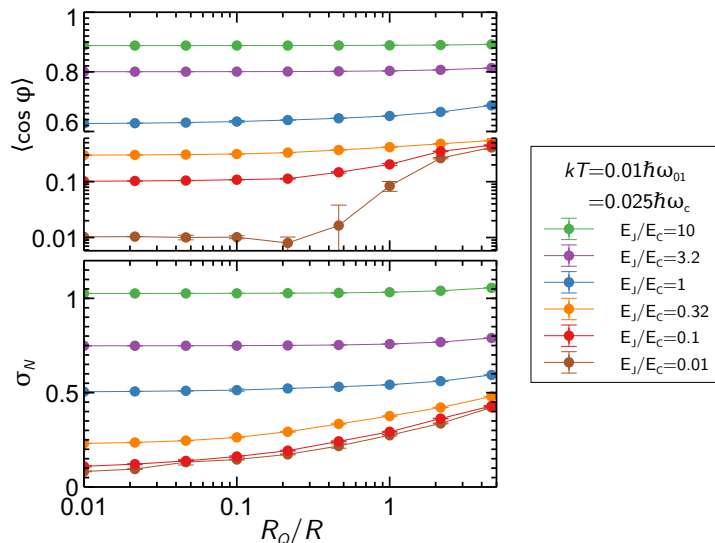


Figure 3. Resistance dependence of  $\langle \cos \varphi \rangle$  (top panel - note the log-lin broken vertical axis) and  $\sigma_N$  (bottom panel) for different  $E_J/E_C$  ratios at the low temperature  $kT = 0.01\hbar\omega_{01}$  and for  $\hbar\omega_c = 0.4\hbar\omega_{01}$ . One observes that both  $\langle \cos \varphi \rangle$  and  $\sigma_N$  increase when reducing the value of the shunt resistance and tend to saturate at the bare CPB value at large  $R$ . No change of behavior is observed around  $R = R_Q$ .

5) yield  $\langle V \rangle \propto \langle N \rangle = 0$  and  $I_0 \langle \sin \varphi \rangle = I_b$  up to numerical accuracy, corresponding to a supercurrent flow through the junction.

## V. DISCUSSION

The superconducting linear response shown in Fig. 5 is consistent with the result obtained from Kubo's theory in IIA. It explains why RSJ experiments [18, 41] may observe signatures of a finite dc supercurrent that saturates at low temperatures for parameters that were previously believed to have an insulating ground state. As said above, a small current bias slightly shifts the global minimum of the potential of the fictitious fluxonium away from  $\varphi = 0$ , but the states remain localized in phase, so that the dc voltage remains zero (this argument is critically examined in Appendix E 5, where we also discuss what eventually limits this superconducting behavior).

Our numerical results show that the  $R \rightarrow \infty$  limit of the RSJ smoothly recovers the well known physics of the CPB family of Josephson qubits, as expected for a vanishing perturbation. In addition, we observe that in the RSJ with a finite shunt resistance, at low temperatures, the effective Josephson coupling  $E_J \langle \cos \varphi \rangle$  saturates to a value larger ( $\geq$ ) than in the bare CPB and the rms charge fluctuations on the capacitor  $\sigma_N$  saturate to values larger ( $\geq$ ) than in the bare CPB, and strictly larger than in the  $C||Y$  circuit, for all the parameters we tested. This establishes that, in the Caldeira and Leggett model with an Ohmic environment having a finite UV cutoff frequency, the shunted Josephson junction's ground state is superconducting and actually *more superconducting* than the bare CPB junction. Notably, when  $E_J \ll E_C$  one has  $E_J \langle \cos \varphi \rangle \rightarrow E_J^2/E_C$  in the CPB, setting a lower bound to the RSJ's superconductivity at equilibrium.

Our results further show that the JJ's low- $T$  superconductivity increases at large cutoff of the Ohmic bath. The observed trend is actually simply explained by the counter-term localizing the phase more and more tightly (since  $E_L \propto \omega_c$ ), which would ultimately yield a perfectly localized classical phase at  $\varphi = 0$  (and thus  $\langle \cos \varphi \rangle = 1$ ) when  $\omega_c = \infty$ . The trend can also be equivalently explained by the logarithmic increase with  $\omega_c$  of  $\sigma_{N,C||Y}$  (Eq. (24)), the environment-induced charge fluctuations on the capacitor, which provides more charges states for the Josephson coupling mechanism, driving up both  $\sigma_N$  and  $\langle \cos \varphi \rangle$  (eventually reaching 1). Hence, we conclude a Markovian bath would yield a classical phase JJ with the maximal effective Josephson coupling  $E_J \langle \cos \varphi \rangle = E_J$ , for all values of the resistance. Although this result can be understood simply, it has not been realized so far, to the best of our knowledge. Indeed, in the literature that predicted that transition, it is widely assumed that a strictly Ohmic bath with no UV cutoff would be appropriate for predicting the RSJ ground state (yet, not finding a fully localized phase, for reasons explained below). This assumption that the bath's UV cutoff would be irrelevant is most likely due to assuming that

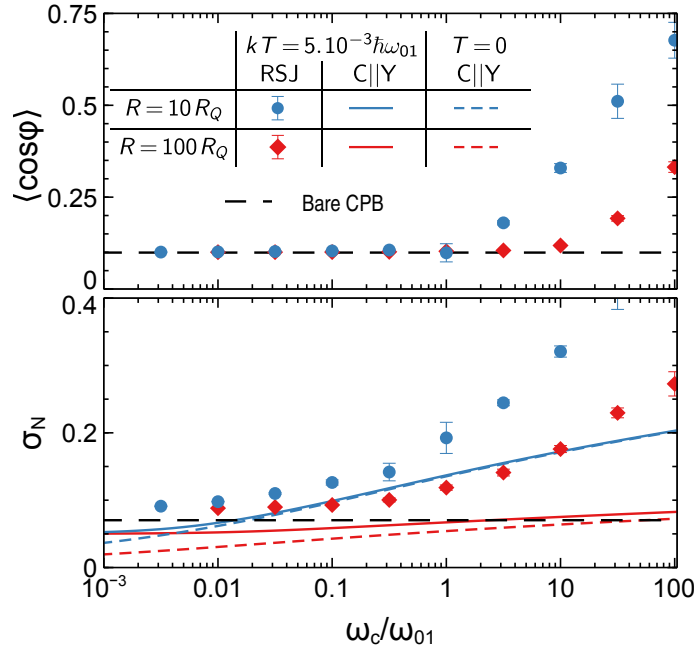


Figure 4. Dependence of  $\langle \cos \varphi \rangle$  (top panel) and  $\sigma_N$  (bottom panel) with the cutoff frequency  $\omega_c$  of the Ohmic bath, for an RSJ with  $E_C = 10E_J$ ,  $R = 10R_Q$  (blue) or  $R = 100R_Q$  (red) at the low temperature  $kT = 0.005\hbar\omega_{01}$ . The black dashed lines correspond to the predicted values for the ground state of the bare CPB. In the bottom panel the colored lines show the predicted charge fluctuations  $\sigma_{N,C||Y}$  in absence of junction conduction, both at the simulated temperature (solid lines) and  $T = 0$  (dashed lines). One observes that at low cutoff the expectation values tend to those of the CPB independently of  $\omega_c$  while at large cutoff the expectation values depend on  $\omega_c$ , with the superconducting character of the junction increasing with  $\omega_c$ .

the junction's capacitance by itself would sufficiently squash the high frequency fluctuations in the system. However, this is not the case since charge fluctuations on the capacitor of an RC circuit diverge at infinite cutoff (see Eq. (24)), and even more so when adding a junction in parallel.

Our findings can be globally explained qualitatively by arguing that connecting a resistor to a CPB can significantly affect the ground state of this nonlinear oscillator only if the environment impedance  $Z(\omega) = Y^{-1}(\omega)$  is comparable to or lower than the effective impedance of the unshunted CPB at its plasma frequency, such that it can reduce the phase fluctuations across the junction. If furthermore the phase fluctuations of the bare CPB are initially large ( $E_C \ll E_J$ ) the reduction of the phase fluctuations due to the resistor leads to an increase of  $\langle \cos \varphi \rangle$ , reducing the junction's effective inductance  $L_{\text{eff}} = \varphi_0^2/E_J \langle \cos \varphi \rangle$ , and hence its effective impedance, which in turn bootstraps the reduction of the phase fluctuations. Here, the method yields the exact self-consistent solution for these environment-modified fluctuations and the corresponding effective Josephson coupling  $E_J \langle \cos \varphi \rangle$ ; this can be seen as generalizing approaches restricted to Gaussian phase fluctuations (see e.g. Ref. [42]) and that predict an effective coupling  $E_J e^{-\frac{1}{2}\langle \varphi^2 \rangle}$  [43]. The linear impedance of the bare CPB can be estimated using

$$\frac{Z_{\text{CPB}}}{R_Q} \sim \frac{1}{2\pi} \sqrt{\frac{\langle \varphi^2 \rangle}{\langle N^2 \rangle}}$$

which would be exact for the harmonic oscillator, or as

$$\frac{Z_{\text{CPB}}}{R_Q} \sim \frac{1}{R_Q} \sqrt{\frac{L_{\text{eff}}}{C}} = \frac{1}{2\pi} \sqrt{\frac{2E_C}{E_J \langle \cos \varphi \rangle}}$$

both of which evolve from  $\frac{1}{2\pi} \sqrt{\frac{2E_C}{E_J}} < 1$  when  $E_C \ll E_J$  to  $\propto \frac{E_C}{E_J} \gg 1$  when  $E_C \gg E_J$ . This roughly explains at which resistance value the upturn of  $\langle \cos \varphi \rangle$  occurs in Fig. 3. Yet, for  $E_J/E_C \ll 1$ , resistances much larger than the above estimates of the CPB linear impedance already induce a substantial change of  $\sigma_N$  compared to the bare CPB, an effect dependent on the cutoff  $\omega_c$  (See Fig. 4).

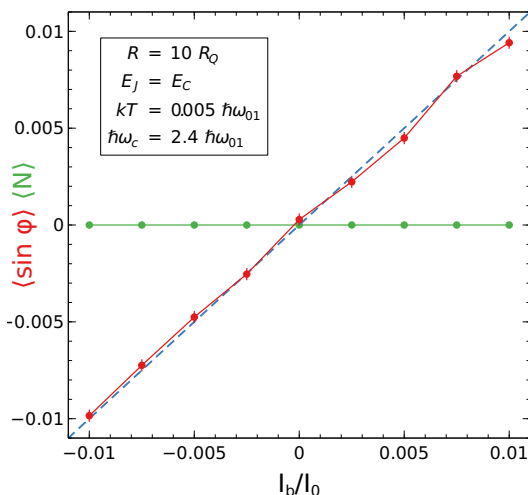


Figure 5. Example linear response expectations values of the current  $I_0 \sin \varphi$  through the junction and the charge  $2eN$  on the capacitor (proportional to the voltage across the junction) when adding a small bias current  $I_b \ll I_0$  to the system. With a resistance  $R = 10R_Q$ , the junction would be in Schmid’s “insulating phase”, while we obtain a superconducting response, in agreement with Kubo’s theory (see II A).

The temperature dependence of  $\langle \cos \varphi \rangle$  is strikingly non-monotonic for  $E_J \ll E_C$  (see Fig. 2). Starting from low temperatures, it first shows a plateau corresponding to the zero point fluctuations, followed by an increase with a local maximum around  $kT/\hbar\omega_{01} = 0.1$ , before reducing and finally vanishing at high temperatures. We believe that this temperature dependence of  $\langle \cos \varphi \rangle$  explains the non-monotonic variation observed in the experimental results of Ref. [18]. The measured scattering amplitude (see Fig. 3 and Appendix E in Ref. [18]) in that experiment is

$$|S_{21}|^2 \propto \frac{1}{|1 + RY_J(\omega_{\text{meas}})|^2} = \frac{1}{1 + \left(\frac{R}{R_Q} \frac{E_J^{\text{sq}}(\Phi)}{\hbar\omega_{\text{meas}}} \langle \cos \varphi \rangle\right)^2},$$

where we assume that the junction’s admittance  $Y_J(\omega) \simeq 1/iL_{\text{eff}}\omega$  is dominated by its inductive behavior at the measurement frequency  $\omega_{\text{meas}}/2\pi \simeq 1$  GHz, with, according to (7),  $L_{\text{eff}}^{-1} = E_J^{\text{sq}}(\Phi)\langle \cos \varphi \rangle/\varphi_0^2$  and  $E_J^{\text{sq}}(\Phi) = E_{J\text{max}}|\cos(\pi\Phi/\Phi_0)|$  the Josephson coupling of the experiment’s SQUID (assumed symmetric), tuned by the applied magnetic flux  $\Phi$ . A precise fitting of the experimental data with the above expression is unrealistic because the measured scattering amplitudes were uncalibrated [18] and the cutoff frequency of the resistive environment was not controlled (it was not known to be a relevant parameter at the time). Yet, plugging  $\langle \cos \varphi \rangle$  for  $E_J/E_C = 0.1$  as computed in Fig. 2, and the experimental parameters  $RE_{J\text{max}}/R_Q\hbar\omega_{\text{meas}} \sim 5 - 10$  in the above expression would already qualitatively capture the variations of the experimental data (at temperatures sufficiently below  $T_c \sim 1.2$ K of Al), with, notably, the temperature of the local maximum admittance (minimum  $|S_{21}|^2$ ) in the experiment that reasonably corresponds to  $kT = 0.1\hbar\omega_{01} \simeq 0.1E_C$  for both samples. This shows our path integral approach enables detailed quantitative comparison with future tailored experiments.

As fully expected from the qualitative argument on the existence of a localized ground state for all parameters given in Sec. III, our numerical results show no sign of Schmid’s dissipative QPT in JJs. In particular, we observe no change of behavior at or near  $R = R_Q$ . As well, equilibrium observables related to transport do not follow power laws of the temperature in the critical region of the expected QPT, which would be the numerical signature of that QPT [19].

In Appendix E we show that the symmetries of the Hamiltonian (which, surprisingly, have not been thoroughly worked out earlier) by themselves also preclude the existence of Schmid’s QPT. We notably reveal that the ground state of the system is infinitely degenerate, such that it does not actually possess a well-defined symmetry that a QPT could break, unlike in the akin spin-boson problem. This degeneracy also manifests itself in a rigorously flat quasicharge ground band (contrary to what is frequently assumed in the literature). The predicted insulating state was supposed to consist of the system trapped at a local minimum of that band (*i.e.* the exact dual of the dc Josephson effect); the flat band forbids it.

Having invalidated Schmid’s prediction in several independent ways, we still need to explain why the entire previous theoretical literature on that question confirmed the prediction. As can be expected, the reason is rather subtle; we show in App. D 2 that it involves two unfulfilled implicit assumptions. The first assumption, already mentioned

above, is that the bath's UV cutoff would be irrelevant, leading to directly consider an infinite cutoff. The second implicit assumption is that this infinite cutoff limit would commute nicely with other limits, but we reveal it does not, yielding results that are nonphysical for this model. The flawed results obtained that way ultimately led to the belief that the RSJ and the 1D quantum impurity problem are equivalent, which we dispel (see App. D4). Our work shows that, contrary to the past literature, it is essential to take into account the finiteness of resistor's UV cutoff (and the ensuing non-Markovian dynamics) for predicting the superconducting RSJ ground state correctly (with its fluctuations), whatever the theoretical approach; it is not just a matter of taste or convenience.

Finally, the present work provides for the first time a reliable way of predicting the equilibrium behavior of JJs in presence of arbitrary linear environments –even frequency-dependent ones–, provided the impedance is not too small. In the opposite small shunting impedance regime, the approach should be doable in the dual picture, considering the coupling of the JJ charge with the impedance's fluctuating voltage.

## VI. CONCLUSIONS

In this work we prove that the Caldeira-Leggett Hamiltonian used to model a resistively shunted Josephson junction has no superconducting-to-insulating quantum phase transition, contrary to what was widely believed after Schmid's 1983 prediction. We actually provide three independent demonstrations relying respectively on Kubo's linear response theory, symmetry arguments, and an exact path integral method.

Our path integral approach lends itself to a numerical implementation yielding the equilibrium reduced density matrix and the expectation values of observables of the RSJ. This provides the first workable method to predict quantitatively the behavior of the RSJ in a wide range of parameters where predictions were previously impossible or incorrect. The method handles arbitrary frequency-dependent environment impedances, and, in principle, it can be extended to dynamical situations.

Our results

- fully support the conclusions of Murani *et al.* [18] that a resistive shunt with  $R > R_Q$  does not render a Josephson junction *insulating*. Actually, a shunt resistor can only make a junction *more superconducting* than it would be in its absence.
- recover the CPB physics when the shunt resistance is made very large, as expected for a vanishing perturbation,
- reveal an unforeseen dependence of the junction's superconducting properties with the resistor's UV cutoff, which must therefore be taken into account for making sensible predictions for the RSJ.

Our work reveals and clarifies several subtle issues that led to the flawed prediction and its long trail in the literature. Namely, we

- point to an issue of non-commuting limits when considering a resistor with infinite cutoff from the onset,
- explain why the RSJ and the 1D quantum impurity problem are not analogous (the latter having a QPT, indeed), contrary to what was previously thought,
- clarify the symmetries and degeneracies of the phase states in the RSJ, a theoretical question that has also long been a matter of debate in the community.

## VII. ACKNOWLEDGMENTS

We are grateful to H. Grabert, J. Stockburger, C. Ciuti, L. Giacomelli, F. Borletto, R. Riwar, N. Roch, X. Waintal, I. Snyman, M. Houzet, O. Maillet, S. Latil, C. Gorini and our colleagues of the Quantronics group at CEA-Saclay for stimulating discussions, comments and helpful inputs at various stages of this work initiated 7 years ago. This work is supported in part by ANR project Triangle ANR-20-CE47-0011-02.

## APPENDICES

### Appendix A: On the interpretation of Schmid's QPT in Josephson junctions

What Schmid saw as remarkable in his work [3], was the *localization effect* in one well at large enough friction. Indeed, at low friction, a delocalized particle was seen as no surprise since one expects to recover Bloch states in the vanishing friction limit.

However, the way in which Schmid's analogy was received by physicists familiar with the Josephson junction had a totally reversed "surprise factor" : The predicted localized JJ phase was seen as run-of-the-mill since it seems just like the classical description of the JJ which the beginner first learns. On the contrary, the delocalized phase in the weak damping limit, which was the vanilla situation for Schmid's original particle, became an extraordinary situation in which the JJ would turn *insulating* under the action of the resistance, even when the corresponding friction force is vanishing, implying one must give up the notion of a perturbative effect. As well, according to what became the standard interpretation of Schmid's analogy, *a JJ could only be superconducting when it experienced strong damping of its phase*, even if this was at odds with the well-understood classical limit of the device in which dissipation is not *needed* to have a superconducting device and which well explained abundant experimental observations of supercurrents in large underdamped, junctions (by far the easiest to make and measure). In addition of conflicting with perturbation theory and the classical limit, Schmid's prediction was also at odds with the theoretical work that had already been done on the RSJ [44–46], and which Caldeira and Leggett had completed. Notably, Caldeira and Leggett's work quantitatively accounts for experiments on RSJs [2], and there is no trace of Schmid's QPT in their tunneling rate.

### Appendix B: Generation of discrete noise increments with required correlations

For the Lorentzian  $\text{Re}Y(\omega)$  Eq. (8) we assume, the integral in (16) converges for  $0 < \tau < \hbar\beta$  and admits the analytical solutions

$$\begin{aligned} \mathcal{C}_{II}(-i\tau) &= \frac{\hbar}{\pi R} \omega_c^2 \left( \text{Re} \left[ e^{-\frac{2i\pi\tau}{\beta\hbar}} \Phi \left( e^{-\frac{2i\pi\tau}{\beta\hbar}}, 1, \frac{\beta\hbar\omega_c}{2\pi} + 1 \right) \right] + \frac{\pi}{\beta\hbar\omega_c} \right) \\ &= \sum_{n=0}^{\infty} \mathcal{C}_n \cos(\omega_n \tau) \end{aligned} \quad (\text{B1})$$

where  $\Phi$  is the Lerch transcendent function,  $\omega_n = n \frac{2\pi}{\beta\hbar}$ , and

$$\mathcal{C}_n = \frac{\hbar}{R} \omega_c^2 \frac{(2 - \delta_{n0})}{\beta\hbar\omega_c + 2\pi n}. \quad (\text{B2})$$

The expressions in (B1) are even and  $\hbar\beta$ -periodic in  $\tau$  (and, of course, symmetric about  $\tau = \hbar\beta/2$ ). At  $\tau \sim 0$  these expressions have a mild divergence  $\mathcal{C}_{II}(-i\tau) \sim R^{-1} \omega_c^2 \log |\tau|$  (See Fig. 6). Note that other forms of  $\text{Re}Y(\omega)$  with a sharper cutoff, such as e.g.  $\text{Re}Y(\omega) = \exp(-|\omega|/\omega_c)/R$ , even yield a finite  $\mathcal{C}_{II}(0)$ , *i.e.* a finite variance for  $\xi(\tau)$  at all times. This should clear possible worries associated with the mild divergence of  $\mathcal{C}_{II}$  in the Lorentzian case, since one expects that the overall behavior of a system should not depend on the precise shape of such cutoff.

For satisfying Eq. (17), the random noise  $\xi(\tau_n)$  can be naively drawn as the real numbers

$$\xi(\tau_n) = \sum_{m=0}^{M-1} R_m \cos(\omega_m \tau_n + \theta_m) \quad (\text{B3})$$

where  $\theta_0 = 0$ ,  $R_0$  is a normally-distributed random number with zero mean and variance  $\mathcal{C}_0$ , and the  $\{R_{m>0}\}$  are taken fixed as  $R_{m>0} = \sqrt{2\mathcal{C}_m}$ , with the  $\{\theta_{m>0}\}$  random and uniformly-distributed in  $[0, 2\pi)$ . Then, the  $\{\xi(\tau_n)\}$  ensemble (Eq. (B3)) is efficiently obtained as the real part of the fast Fourier transform (FFT) of  $\{e^{i\theta_m} R_m\}$ . With

this construction, the correlators are

$$\begin{aligned}
\langle \xi(\tau_n)\xi(\tau_m) \rangle &= \sum_{j,k=0}^{M-1} \langle R_k R_j \cos(\omega_k \tau_n + \theta_k) \cos(\omega_j \tau_m + \theta_j) \rangle \\
&= \sum_{j,k=0}^{M-1} \frac{1}{2} \{ \langle R_k R_j \cos(\delta\tau \delta\omega(jm - kn) - \theta_k + \theta_j) \rangle \\
&\quad + \langle R_k R_j \cos(\delta\tau \delta\omega(kn + jm) + \theta_k + \theta_j) \rangle \} \\
&= \langle R_0^2 \rangle \frac{1}{2} + \sum_{j=1}^{M-1} R_j^2 \frac{1}{2} (\cos(\delta\tau \delta\omega j(m-n))) + \langle R_0^2 \rangle \frac{1}{2} \cos(2\theta_0) \\
&= \sum_{j=0}^{M-1} \mathcal{C}_j \cos(j(m-n)\delta\tau\delta\omega) \\
&= \mathcal{C}_{II}(-i(\tau_n - \tau_m)) - \sum_{j=M}^{\infty} \mathcal{C}_j \cos(j(m-n)\delta\tau\delta\omega) \tag{B4}
\end{aligned}$$

which almost fits the requirement (Eq. (17)).

The first problem with this naive algorithm is the logarithmic divergence of  $\mathcal{C}_{II}(-i\tau)$  at  $\tau = 0$ , for the Lorentzian  $\text{Re}Y(\omega)$  we consider. This is solved by taking, instead of  $\mathcal{C}_{II}(-i(\tau_n))$ , the averaged  $\bar{\mathcal{C}}_{II}(-i(\tau_n)) = \delta\tau^{-1} \int_{\tau_n - \delta\tau/2}^{\tau_n + \delta\tau/2} \mathcal{C}_{II}(-i\tau_n) d\tau$  over the time steps of our discretization, which removes the weak divergence. This amounts to filtering the correlation function by convolving it by a rectangular function, and hence to multiply the Fourier coefficients  $\mathcal{C}_n$  by a sinc

$$\mathcal{C}_n \rightarrow \bar{\mathcal{C}}_n = \mathcal{C}_n \text{sinc} \frac{\delta\tau}{2} \omega_n = \mathcal{C}_n \text{sinc} \frac{n\pi}{M},$$

and to define the  $\{R_m\}$  from these  $\{\bar{\mathcal{C}}_m\}$ .

Even with such filtering, a second problem remains : when taking the FFT, we only sum the  $M$  first Fourier coefficients so that the correlator we obtain deviates from the ideal value, as apparent in Eq. (B4). When  $M$  is large enough, this deviation leaves a noticeable systematic error only for the same-time correlator

$$\langle \xi(\tau_n)\xi(\tau_n) \rangle = \bar{\mathcal{C}}_{II}(0) - \Delta$$

where the error  $\Delta$  is

$$\Delta = \sum_{j=M}^{\infty} \bar{\mathcal{C}}_j = \frac{\hbar}{R} \omega_c^2 \frac{M \text{Im} \left( \Phi \left( e^{-\frac{i\pi}{M}}, 1, M \right) - \Phi \left( e^{-\frac{i\pi}{M}}, 1, M + \frac{\beta\hbar\omega_c}{2\pi} \right) \right)}{\pi\beta\hbar\omega_c}.$$

Such Dirac delta-like error can be easily corrected by applying a shift to all the Fourier coefficients entering our FFT, except the zero-frequency one which provides the correct baseline

$$\bar{\mathcal{C}}_j \rightarrow \tilde{\mathcal{C}}_j = \bar{\mathcal{C}}_j - (1 - \delta_{0j}) \frac{\Delta}{M-1}, \quad j = 0, \dots, M-1.$$

The  $\{R_m\}$  are finally evaluated from the  $\{\tilde{\mathcal{C}}_m\}$  in place of the initial  $\{\mathcal{C}_m\}$ . With these corrections made, we compare the numerical correlations to the expected  $\bar{\mathcal{C}}_{II}(-i(\tau))$  in Fig. 6

### Appendix C: Basis states, operator matrices and thermal expectation values for the bare CPB

In this appendix we evaluate thermal expectations values of some operators of the CPB, working in the eigenbasis. The CPB eigenstates can easily be obtained numerically in a truncated discrete charge basis, but below we rather obtain them analytically in terms of Mathieu functions [47, 48].

The Shrödinger differential equation for the bare CPB Hamiltonian in absence of offset charge is

$$E_C \Psi''(\varphi) - (E_J \cos\varphi) \Psi(\varphi) = E \Psi(\varphi). \tag{C1}$$

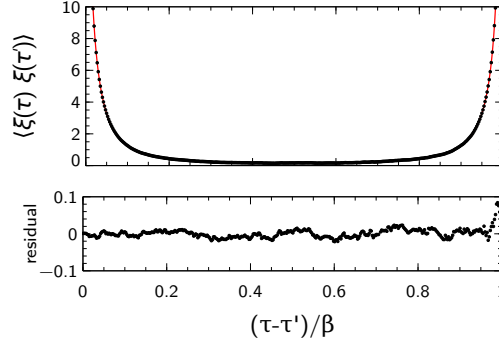


Figure 6. Comparison of the filtered (see text) theoretical current noise correlator in imaginary time for a Lorentzian  $\text{Re}Y(\omega)$  (red continuous line) and experimental correlator for  $10^6$  drawings of a noise sequence (black dots). The bottom panel shows the difference between the numerical correlator and its expected value. Parameters are  $R = 3R_Q$ ,  $\beta\hbar\omega_c = 30$ , 401 time steps.

This equation is a form of Mathieu's equation

$$f''(z) + (a - 2q \cos 2z)f(z) = 0,$$

whose solutions are known as special functions [49]. Furthermore, given that the potential is periodic in  $\varphi$ , Bloch's theorem implies the eigenfunctions of (C1) are of the form

$$\Psi_{np}(\varphi) = \langle \varphi | n, p \rangle = e^{ip\varphi} u_{np}(\varphi),$$

where  $n$  is a band index, and  $p$  is the quasicharge (i.e. Bloch's quasimomentum), with  $u_{np}(\varphi)$  a  $2\pi$ -periodic function of  $\varphi$  (same period as the  $\cos \varphi$  potential). If the CPB is not connected to anything,  $p$  is fixed to zero, whereas when connected to a circuit that can let charge circulate,  $p$  can fluctuate and take any value in  $\mathbb{R}$ .

Using knowledge from the solutions of Mathieu's equation, the eigenenergy  $E_{np}$  of  $\Psi_{np}(\varphi)$  is given by

$$E_{np} = \frac{E_C}{4} \lambda_{\chi(n,p)}(-2E_J/E_C),$$

where  $\lambda_\nu$  denotes the *Mathieu characteristic value* special function indexed by its *characteristic exponent* and

$$\chi(n, p) = n + n \bmod 2 + (-1)^n 2 |\text{frac}(p)|$$

is a function giving the characteristic exponents, such that the eigenenergies are sorted increasing with the band index  $n \in \mathbb{N}$ , and where the fractional value  $\text{frac}(p) = p - \text{round}(p)$ , with  $\text{round}(p)$ , rounding to the nearest integer. The  $u_{np}$  functions themselves can be expressed as

$$u_{np}(\varphi) = \frac{e^{-ip\varphi}}{\sqrt{2\pi}} \left( \text{ce}_{\chi(n,p)} \left( \frac{\varphi}{2}, -2\frac{E_J}{E_C} \right) + i(-1)^n \text{sign}(\text{frac}(p)) \text{se}_{\chi(n,p)} \left( \frac{\varphi}{2}, -2\frac{E_J}{E_C} \right) \right),$$

where the Mathieu  $\text{ce}_\nu$  and  $\text{se}_\nu$  are respectively even and odd real functions of  $\varphi$  [49]. Note that  $\lambda_\nu$  has discontinuities when  $\nu = \chi(n, p)$  is strictly an integer (i.e. when  $2p$  is an integer), as well as either  $\text{ce}_\nu$  or  $\text{se}_\nu$ ; the eigensolutions to consider at these values in each band are then obtained as the limits when approaching the discontinuity. Our expressions with Mathieu special functions extend those of Ref. [47] to all quasicharges values, but differ from those of Ref. [48].

It is then straightforward to obtain the matrix elements of  $N = -i\frac{\partial}{\partial\varphi}$  and  $N^2$ ,

$$\begin{aligned} \langle n, p | N | n', p' \rangle &= \delta(p - p') \left( \delta_{nn'} p - i \int_0^{2\pi} d\varphi u_{np}^*(\varphi) \frac{du_{n'p}(\varphi)}{d\varphi} \right), \\ \langle n, p | N^2 | n', p' \rangle &= \delta(p - p') \left( \delta_{nn'} p^2 - 2ip \int_0^{2\pi} d\varphi u_{np}^*(\varphi) \frac{du_{n'p}(\varphi)}{d\varphi} \right. \\ &\quad \left. - \int_0^{2\pi} d\varphi u_{np}^*(\varphi) \frac{d^2 u_{n'p}(\varphi)}{d\varphi^2} \right), \end{aligned}$$



and those of any function  $f(\varphi)$  are

$$\langle n, p | f(\varphi) | n', p' \rangle = \delta(p - p') \int_0^{2\pi} d\varphi f(\varphi) u_{np}^*(\varphi) u_{n'p}(\varphi).$$

Finally, we can evaluate thermal equilibrium expectation values from the thermal density matrix  $\rho_\beta = e^{-\beta H} / \text{Tr} e^{-\beta H}$  and the matrix elements of operators as

$$\langle A \rangle = \text{Tr} \rho_\beta A = \sum_n \int_{-1/2}^{1/2} dp e^{-\beta E_{np}} \langle n, p | A | n, p \rangle.$$

In qubits, the quasicharge charge  $p$  has values externally imposed by the gate. The low impedance of the gate voltage is such that  $p$  is nearly fixed and one should then only sum over the band index. On the other hand, if the qubit's "island" is not connected to a gate capacitance but rather to an element that can let charge circulate,  $n_g$  can fluctuate and take any value. In Fig. 7, assuming either fixed charge offset or that  $p$  (or  $n_g$ ) can take any value, we plot the thermal expectation values  $\sigma_N = \langle N^2 \rangle^{1/2}$  of the rms fluctuations of the charge  $N$ , and the Josephson coherence factor  $\langle \cos \varphi \rangle$ , which, being non-zero, are both indicators of the superconducting character of the unshunted CPB. One could also consider  $\langle \sin^2 \varphi \rangle = (1 - \langle \cos 2\varphi \rangle)/2$ , the fluctuations of the supercurrent, which is 1/2 when the junction is insulating ( $\varphi$  is delocalized, with all values equally probable) and smaller than 1/2 when the junction has finite supercurrent fluctuations ( $\langle \sin^2 \varphi \rangle = 0$  for the classical superconducting junction in absence of phase bias).

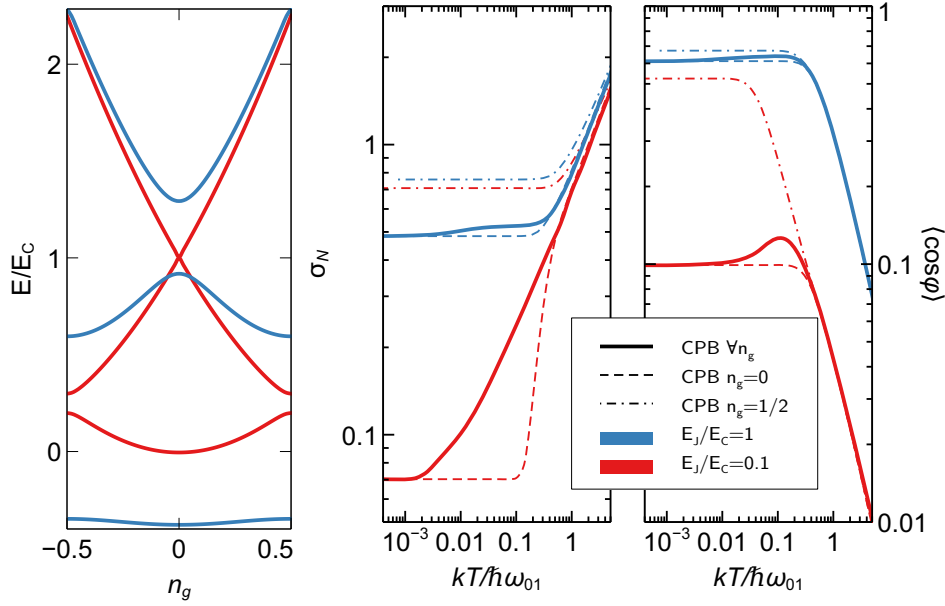


Figure 7. For all panels, red:  $E_J = 0.1E_C$ , blue:  $E_J = E_C$  and  $\hbar\omega_{01} = E_1(n_g = 0) - E_0(n_g = 0)$ . Left panel: energy bands  $E_0$ ,  $E_1$  and  $E_2$  (from bottom to top) of the CPB as a function of the gate charge. Middle (resp. right) panel, thermal expectation values of rms fluctuations of the charge  $N$  (resp. Josephson coherence factor  $\langle \cos \varphi \rangle$ ) as a function of temperature, for fixed gate charge  $n_g = 0$  (thin dashed lines),  $n_g = 1/2$  (thin dashed-dot lines), or (thick full lines) when allowing all gate charges.

This figure shows that at high temperatures, when  $kT \gtrsim \hbar\omega_{01}$  (temperature larger than the separation of the first two bands at  $n_g = 0$ ), the expectation values follow power laws  $\sigma_N = \sqrt{kT/2E_C}$  and  $\langle \cos \varphi \rangle \propto T^{-1}$ , with values independent of whether  $n_g$  is kept fixed or allowed to vary. In the opposite low temperature limit where  $kT \ll E_0(n_g = 1/2) - E_0(n_g = 0)$  (the amplitude of the ground quasicharge band), expectation values saturate to a plateau corresponding to the zero point fluctuations of the ground state at  $n_g = 0$ . For  $E_J \ll E_C$ , these zero point values are  $2\sigma_N^2 = \langle \cos \varphi \rangle \simeq E_J/E_C$ .

In the intermediate temperature range, allowing charge fluctuations on the capacitor enhances both  $\sigma_N$  and  $\langle \cos \varphi \rangle$  with respect to the fixed  $n_g = 0$  case, and this effect is most pronounced when  $E_C/E_J$  is large (deep ground quasicharge band). For  $\langle \cos \varphi \rangle$ , this notably leads to a striking non-monotonic  $T$ -dependence, with a local maximum

at  $kT \sim 0.1\hbar\omega_{01}$ . This maximum is easily explained. In JJs with  $E_C \gg E_J$ , Cooper pair transfer occurs mostly through a second order tunneling process of quasiparticles, with a virtual intermediate state on higher charge parabolas. When allowing thermal fluctuations of the quasicharge away from 0 in the ground band, the energy difference between the ground and the lowest virtual excited state is reduced, hence increasing the effective Josephson coupling. At temperatures  $kT \sim \hbar\omega_{01}$  or higher, the excited bands also get populated which then reduces the effective Josephson coupling.

## Appendix D: Comparing our work to the literature

### 1. Effective actions

The basis of our approach is the same as that used in most of the literature on Schmid's transition. Starting from the Caldeira-Leggett Hamiltonian (1) the dissipative bath is traced out using the Feynman-Vernon influence functional to obtain an effective action, from which one infers the properties of the system. However, several choices are possible, leading to different writings for the effective action in different works. Here, we show that we are describing the physics of the RSJ on the same grounds as in the rest of the literature on Schmid's transition, although with a more general kernel in the influence functional.

The total action for the system with the bath influence functional we consider, before performing the Hubbard-Stratonovich transformation, is (Eq. (12-13))

$$S_{\text{FI}}^E[\varphi] + \Phi[\varphi] = \int_0^{\hbar\beta} d\tau \left( \frac{\hbar^2}{4E_C} \dot{\varphi}^2 - E_J \cos \varphi + E_L \varphi^2 \right) - \frac{1}{2} \int_0^{\hbar\beta} d\tau \int_0^{\hbar\beta} d\tau' \varphi(\tau) K(\tau - \tau') \varphi(\tau'), \quad (\text{D1})$$

with the kernel  $K$  given by Eqs. (16) and (B1). In the review Ref. [9], Schön and Zaikin write the effective action for the RSJ as

$$S[\varphi] = \int_0^{\hbar\beta} d\tau \left( \frac{\hbar^2}{4E_C} \dot{\varphi}^2 - E_J \cos \varphi \right) + \frac{1}{4} \int_0^{\hbar\beta} d\tau \int_0^{\hbar\beta} d\tau' K_\infty(\tau - \tau') (\varphi(\tau') - \varphi(\tau))^2 \quad (\text{D2})$$

(converting their notations to ours) where the first integral is the action of the Cooper pair box (with no counter-term) and where the kernel  $K_\infty(\tau)$  has the form

$$K_\infty(\tau) = \frac{R_Q}{2R} \frac{\hbar}{\left( \hbar\beta \sin \frac{\pi\tau}{\hbar\beta} \right)^2} = \lim_{\omega_c \rightarrow \infty} K(\tau), \quad (\text{D3})$$

which corresponds to the particular case where the kernel Eq. (16) is evaluated with a purely Ohmic admittance  $\text{Re}Y(\omega) = 1/R$ , without any UV cutoff (*i.e.* taking  $\omega_c = \infty$  in (8)). The action used by Schmid [3] is the same as (D2), with the influence kernel being furthermore the zero temperature limit of (D3). For a moment, let us consider the influence functional of (D2) with the more general kernel  $K$  in place of  $K_\infty$ , and expand the square of phase difference. Then, using the facts that  $K$  is even and periodic and that  $\int_0^{\beta\hbar} d\tau K(\tau) = 2E_L$ , one indeed formally recovers our form of the action with the counter-term,

$$\begin{aligned} \frac{1}{4} \int_0^{\beta\hbar} d\tau \int_0^{\beta\hbar} d\tau' K(\tau - \tau') (\varphi(\tau') - \varphi(\tau))^2 &= \int_0^{\beta\hbar} d\tau E_L \varphi(\tau)^2 \\ &\quad - \frac{1}{2} \int_0^{\hbar\beta} d\tau \int_0^{\hbar\beta} d\tau' \varphi(\tau) K(\tau - \tau') \varphi(\tau'). \end{aligned} \quad (\text{D4})$$

Thus, provided one uses the same finite-cutoff kernel (16) in our effective action (D1) and in (D2), the path integrals are equal; in particular, the ground states of these actions coincide. Hence, the localized ground state we find is also a valid ground state for Schmid's action with the finite-cutoff kernel (16). This remains true when taking limits (*e.g.*  $T \rightarrow 0$ ), and in particular for the  $\omega_c \rightarrow \infty$  limit considered by many authors, where we find this localized ground state becomes fully localized in phase (see Sec. V).

For completeness, we present another form of the action in Appendix E 1.

## 2. Why our results contradict previous theoretical work

Even though our path integral equations appear compatible with those used by previous authors confirming Schmid's QPT prediction (see D 1), our equations lead us to conclude the opposite of these authors regarding that QPT. We discuss here more specifically the work of Werner and Troyer (WT) [14], who use the effective action (D2) and apply the path integral quantum Monte Carlo numerical technique to investigate the predicted QPT in the RSJ. Hence, in principle, their technique and ours both calculate numerically the same path integral, and a close examination should reveal why we come to different conclusions regarding the predicted QPT.

First, we observe that in spite of the formal equivalence of our two methods, it is not possible to directly recover and check WT's results with our stochastic Liouville method because, with the infinite cutoff kernel (D3) they use, (i)  $E_L = \frac{1}{2} \int_0^{\beta\hbar} d\tau K(\tau) = \infty$  and (ii) whatever the time discretization chosen, the strong  $\tau^{-2}$  divergence of  $K$  at short times prevents drawing small stochastic increments for a proper numerical integration of the Liouville equation. This unexpected non-equivalence of our two methods in the infinite cutoff limit considered by WT highlights that this limit requires careful handling (something one can hardly do by considering from the onset an infinite cutoff).

Precisely, in Sec. IV and V of the main text, we investigate the role of the bath cutoff  $\omega_c$  and show that, for reasons easily explained, phase fluctuations reduce as  $\omega_c$  increases, eventually reaching a classical phase state in the  $\omega_c \rightarrow \infty$  limit. This trend and this limit we find are the opposite of what would be needed to recover WT's numerical results when  $R > R_Q$ , *viz.* a state with diverging phase fluctuations (see Fig. 3 in [50], the preprint version of [14]). We also find a result opposite to them when we evaluate the linear response as they do (see next subsection D 3, and Fig. 3 of Ref. [14]). We stress that, on our side, we take the limit in a controlled manner and that our results are in agreement with Kubo's linear response, with symmetry considerations, with experiments, and free of the issues mentioned in Appendix A. All the contrary for WT's results which only agree with Schmid's results.

However, we observe that these opposite results are obtained by taking limits differently : in our approach, we first take the low  $T$  limit and then we can consider the infinite cutoff limit, while WT take the same limits in the reverse order. The different outcomes reveal that these two limits do not commute. Highlighting this non-commutation of limits is a key result of our work which enables resolving the conundrum around Schmid's prediction.

In summary, by choosing to use the kernel (D3) in the action (D2), one implicitly assumes (i) an infinite cutoff would correctly describe an actual RSJ experiment, and also supposes (ii) the environment cutoff can be taken to infinity before evaluating the path integral and considering its low temperature limit. Our work reveals that neither of these implicit assumptions holds. These subtle unfulfilled assumptions suffice to explain why the phase delocalization QPT found by WT, (confirming Schmid's results) does not describe the actual physics: it is an uncontrolled, non-physical result in that model of the RSJ. These unfulfilled assumptions impact similarly the results of all the other authors (Schmid, in particular) who consider the same  $\omega_c = \infty$  limit from the onset.

It happens that the (nonphysical) results obtained in this model by first taking the non-commuting  $\omega_c = \infty$  limit coincide with the QPT phenomenology of the 1D quantum impurity problem [16, 17]. Before the present work, it was claimed that these systems were equivalent and this coincidence of results was seen as a strong validation of Schmid's prediction in this model (and the whole literature on it). Below, in D 4, we explain why the 1D systems and the Caldeira-Leggett model of the RSJ are in fact *not* equivalent (one indeed having a QPT, the other, not).

## 3. Evaluating dc mobility using the stochastic Liouville method

In Ref. [14], WT take advantage of the analyticity of  $S_{\varphi\varphi}(\omega)$  to evaluate dc impedance of the RSJ as  $\lim_{\omega \rightarrow 0} (\omega S_{\varphi\varphi}(\omega))$  (see II A) by extrapolating the variations of

$$\mathcal{F}(\omega_1) = \omega_1 S_{\varphi\varphi}(i\omega_1) = \frac{\omega_1}{\hbar} \int_0^{\hbar\beta} \langle \varphi(-i\tau)\varphi \rangle e^{i\omega_1\tau} d\tau \quad (\text{D5})$$

upon reducing the first Matsubara frequency  $\omega_1 = 2\pi kT/\hbar$  [14]. The stochastic Liouville method can also provide the imaginary time correlator  $\langle \varphi(-i\tau_m)\varphi \rangle$  at the discrete time steps  $\{\tau_m = m\delta\tau\}$  (see Sec. III B 1). For a given realization of the random noise  $\xi(\tau)$  and a given intermediate time  $\tau_m$ ,  $\text{Tr} \rho_\xi \varphi(-i\tau_m)\varphi$  is obtained by splitting the discrete integration of the imaginary time evolution in two parts, and inserting the phase operator both at  $\tau_0 = 0$  and at the split  $\tau_m$ , and taking the trace. Finally, as for the RDM, for each intermediate time  $\tau_m$ , one averages over the values obtained for the different realizations of  $\xi$ . In Fig. 8, we carry out the same extrapolation as WT on our numerical results for the imaginary time correlator  $\langle \varphi(-i\tau)\varphi \rangle$ , for  $R = 10R_Q$ . The data clearly point to a vanishing limit for (D5), *i.e.* a superconducting linear response, consistent with the rigorous time-domain result found in II A and all our other results. This contradicts the results in Fig. 3 of WT [14] for  $R > R_Q$  (see discussion above in D 2)

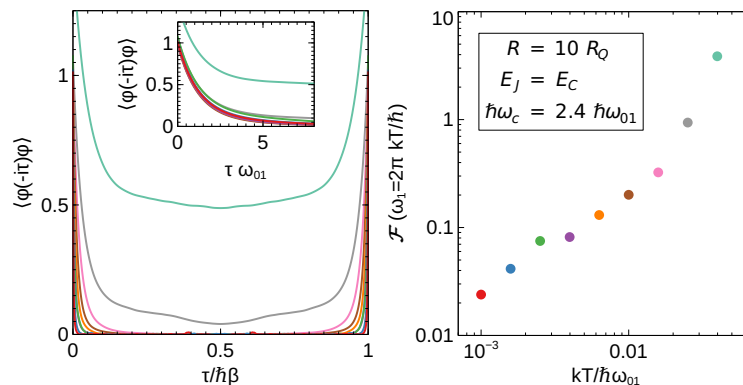


Figure 8. Imaginary time dynamics of the system from stochastic Liouville simulations, for the same RSJ parameters as in Fig. 5. Left panel : imaginary time correlator of the phase, for different temperatures (the temperature of a given curve is the abscissa of the same-colored dot in the right panel). Main panel : full period of the correlator. Inset : short-time close-up with a fixed timescale, showing that the decay of the correlator becomes  $T$ -independent at low temperatures, as the system reaches its ground state. Right panel : evolution of Eq. (D5), calculated with the left panel data. The saturation shown in the left panel inset, makes the integral in (D5) tend to a constant, and thus, up to the uncertainty due to the stochastic method, this quantity varies linearly with the first Matsubara frequency  $\omega_1$  at low temperature, clearly pointing to  $\text{Re } Z(0) = 0$  for the RSJ. When increasing  $\omega_c$ ,  $\langle \varphi\varphi \rangle$  is reduced and this result persists.

#### 4. Why the RSJ differs from 1D quantum impurity problems

In a famous paper [16], Kane and Fisher (KF) showed that a 1D electronic channel with an impurity has a QPT dependent on the Luttinger interaction parameter in the channel, and the scaling laws of the corresponding quantum critical regime were indeed observed experimentally [51–53] in related systems. In their work, by bosonizing the 1D fermions [54, 55], KF derive equations they present as “formally equivalent to the Caldeira-Leggett model for a resistively shunted Josephson junction”, with notably a cosine term similar to the Josephson coupling, and they identify their QPT with Schmid’s QPT. The fact that our present theoretical results exclude a QPT for the RSJ in this model (in agreement with experiment), while the QPT exists both in the theory and experiments on the 1D impurity problem, shows that, actually, the *equivalence* does not hold. Here, we explain why the cosine term they obtain is, in fact, not analogous to the Josephson coupling; it describes a different physics.

The cosine term obtained by KF describes the scattering, by the impurity, of bosonic excitations which act as the dissipative bath in the 1D systems. These excitations are defined only for a non-zero wavevector [54, 55], and thus have a strictly positive energy. Hence, this cosine term has an implicit IR cutoff; notably its matrix element in the ground state of these 1D systems is zero.

On the other hand, in the Caldeira-Leggett Hamiltonian (1) we use to model the RSJ, the  $-E_J \cos \varphi$  term is an effective potential due to coherent tunneling between the BCS ground states on both sides of the junction; as such, it has no IR cutoff. Its argument, the phase  $\varphi$ , is a degree of freedom of the Hamiltonian (1) and, in this model, its amplitude  $E_J$  is considered independent of the dissipative admittance (in Schmid’s paper [3] too, the potential depth is independent of the dissipation) and given by the Ambegaokar-Baratoff value [56]. To be more specific, this term in the Hamiltonian exists with or without a dissipative bath (e.g. in the bare CPB with the Hamiltonian  $H_{\text{CPB}}$  (9)) and it always confers to the junction its inductive (see (4) and Sec. II A), superconducting, behavior. In the presence of the ohmic bath, this  $-E_J \cos \varphi$  potential entails the infinitely degenerate ground state (see App. E). In contrast, in the 1D systems, KF’s cosine term cannot be dissociated from the bath. Its argument is a sum of bath variables which is irrelevant in the ground state; it is thus not an independent degree of freedom characterizing the state of the system, unlike  $\varphi$  in (1). The 1D impurity problem therefore lacks the RSJ ground state properties that ensue from the existence of this degree of freedom (e.g. the inductive response).

Even though we can explain why 1D systems behave differently from the RSJ in spite of deceptively similar-looking equations, it is not clear to us why considering the (non-commuting)  $\omega_c = \infty$  limit from the onset in the RSJ (as Schmid, WT, and most authors did) yields in practice the QPT phenomenology of the 1D systems (see D 2). How come taking this non-commuting limit first (and thus, without control on the results) amounts to unwittingly suppress the degree of freedom  $\varphi$ ? At this point, it seems just an unfortunate coincidence.

## Appendix E: Symmetries and degeneracies in the RSJ

### 1. Phase translation invariance

The Caldeira-Leggett Hamiltonian (1) is left invariant by the discrete translation symmetry that simultaneously shifts the junction's phase and all the bath oscillators' phases by the same multiple of  $2\pi$ :

$$\forall n, \quad \left. \begin{array}{l} \varphi \rightarrow \varphi + 2\pi k \\ \varphi_n \rightarrow \varphi_n + 2\pi k \end{array} \right\} k \in \mathbb{Z}$$

After tracing out the bath oscillators, a translational invariance with respect to the sole junction phase

$$\varphi \rightarrow \varphi + 2\pi k, k \in \mathbb{Z} \quad (\text{E1})$$

must remain for the states of the RSJ obtained from the RDM. Indeed, using (D2) and (D4) one can check this invariance is present in our path integral (11), before the Hubbard-Stratonovich transformation is made. However, the way the Hubbard-Stratonovich transformation is implemented, replacing a quadratic term in  $\varphi$  by a linear term and leading to Eq. (18-19), breaks the above translation invariance. As a result, Eq. (18-19) implicitly select states that are centered at  $\varphi = 0$ . The  $k \neq 0$  translated states would be obtained as solutions of the translated version of Eq. (18-19), where the potential terms in the fictitious system are translated. The effective action we use in the main text thus only yields a subset of the system states, and these localized states are infinitely degenerate through the  $k$  values of this translation.

Although it may seem incorrect at first sight that our localized solutions do not have the translational symmetry built in the original equations, this is neither an error nor a problem. Indeed, it is well known that when the eigenstates of a system are degenerate, some eigenstates may have a lower symmetry than the system as a whole (think *e.g.* of the  $\ell > 0$  orbitals of the hydrogen atom, which do not have the spherical symmetry of the atom's Hamiltonian). A complete basis of the degenerate subspace has the appropriate symmetries.

Let us consider the ground state RDM  $\rho_0 = |\Psi_0\rangle\langle\Psi_0|$  obtained from Eq. (18-19), defining a reduced ground state  $|\Psi_0\rangle$  localized and centered at  $\varphi = 0$  (the diagonal  $\langle\varphi|\rho_0|\varphi\rangle$  of this RDM is the square modulus of the reduced wave function  $\Psi_0(\varphi) = \langle\varphi|\Psi_0\rangle$ , *i.e.* the density of probability of the phase in this ground state). Then, following the above translation arguments, all the translated states  $\{e^{-i2\pi k\hat{N}}|\Psi_0\rangle, k \in \mathbb{Z}\}$  are also valid reduced ground states of the RSJ. From the ensemble of these translated states, one can furthermore construct fully delocalized Bloch states with a dimensionless quasicharge  $q$

$$|\Phi_q\rangle = \mathcal{N} \sum_k e^{-i2\pi k(q+\hat{N})} |\Psi_0\rangle \quad (\text{E2})$$

(with  $\mathcal{N}$  the usual normalization factor of Bloch states) which have the same energy as  $|\Psi_0\rangle$  for all values of  $q$ , and are hence also degenerate ground states. Thus, unlike the CPB, the RSJ has a flat quasicharge ground band, as already stated in Refs. [18, 57] (see also next subsection E 2). The fact that we can exhibit both localized and delocalized ground states illustrates the abstract argument given in Ref. [18], that any valid equilibrium state of the RSJ ought to be representable both as a localized or a delocalized state, based on formal arguments on unitary transformations developed earlier in Ref. [58, 59].

This localized|delocalized duality is further confirmed by the fact that one can come up with different (yet equivalent) equations for that system and which directly yield only delocalized states, for all parameters. Notably, it is possible to transform our effective action (D1) ( $\Leftrightarrow$  Eq. (12-13)) to a mathematically equivalent form :

$$S_{\text{CPB}}^E[\varphi] + \tilde{\Phi}[\varphi] = \int_0^{\hbar\beta} d\tau \left( \frac{\hbar^2}{4E_C} \dot{\varphi}^2 - E_J \cos \varphi \right) - \frac{1}{2} \int_0^{\hbar\beta} d\tau \int_0^{\hbar\beta} d\tau' \varphi(\tau) k(\tau - \tau') \varphi(\tau'), \quad (\text{E3})$$

where the parabolic counter-term potential in the first term has been removed (*i.e.* it is the action of a CPB instead of a fluxonium) and absorbed in the modified influence functional  $\tilde{\Phi}$  (See *e.g.* [33] or [32]). The kernel  $k$  of this modified influence functional is related to the kernel  $K$  (14)-(16) of the influence functional we use in the rest of this work through

$$k(\tau) = K(\tau) - 2E_L \text{III}_{\hbar\beta}(\tau),$$

where the  $\text{III}_{\hbar\beta}(\tau) = \sum_{n=-\infty}^{+\infty} \delta(\tau - n\hbar\beta)$  is the Dirac comb of period  $\hbar\beta$ , such that  $\int_0^{\beta\hbar} d\tau k(\tau) = 0$ . This alternate writing of the effective action does not have the confining potential that localizes our states, and that may seem

artificial to some. After performing the Hubbard-Stratonovich transformation on this effective action, the fictitious system is a particle in a periodic potential submitted to a random noise which causes the particle to diffuse. In equilibrium, the diffusion current must vanish and the probability to find the particle is equal in all the wells. This is confirmed by running the stochastic Liouville method (see Sec. III B) with this counter-term-free modified action, as shown in Fig. 9. We observe that, indeed, without the counter-term, the results resemble the delocalized Bloch states described above, with expectations values of observables matching those of the simulations performed with the counter-term, within the error bars of the simulations. Were the number of wells taken into account in the numerics to be increased, the ground state obtained with this modified kernel would tend to the perfectly periodic phase state  $|\Phi_{q=0}\rangle$  (also known as a compact phase state), as reasoned above.

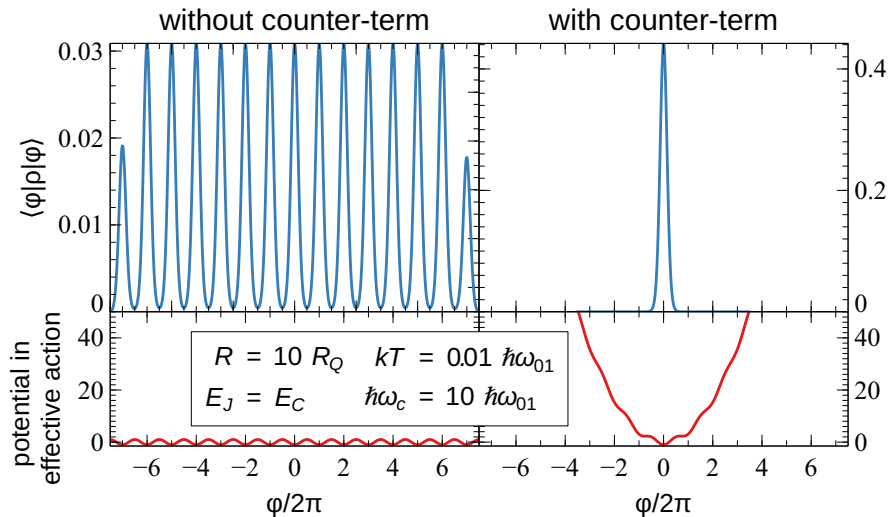


Figure 9. For the same set of parameters given in the label, we compare of the probability density  $\langle \varphi | \rho | \varphi \rangle$  where  $\rho$  is the RDM obtained from the stochastic Liouville method, computed with either (right panels) the effective action with the counter-term (D1) used in this paper, or (left panels) the modified effective action (E3) without the counter-term. The counter-term-free solution is close to a Bloch-like equal-weight superposition of repeated  $2\pi$ -shifted copies of the localized solution obtained with the counter-term, up to edge effects due to the limited number of cosine wells considered in the computation.

An important additional consequence of the translational invariance (E1) of the effective action is that quantities that are actually measurable on that system can only involve  $2\pi$ -periodic functions of  $\varphi$ . Thus, the phase itself, and all its moments, are *not* measurable.

## 2. Charge translation invariance

A unitary transformation  $U = \exp(i\varphi \sum_n N_n)$  applied to the Caldeira-Leggett Hamiltonian (1) yields the so-called charge gauge Hamiltonian  $E_C (N - \sum_n N_n)^2 - E_J \cos \varphi + H_{\text{bath}}$ . The later Hamiltonian is invariant upon a translation of  $N$  and any of the bath  $N_n$  by the same arbitrary amount  $\in \mathbb{R}$ . Similarly to the phase translations, this means that, after tracing out the bath, for the reduced ground state  $|\Psi\rangle$  obtained from the ground state RDM, any charge-translated copy  $e^{iq\varphi}|\Psi\rangle$ ,  $q \in \mathbb{R}$  is also a valid reduced ground state, with the same observables. This is another way to establish the degeneracy of the ground states with respect to the quasicharge, i.e. the flatness of the quasicharge ground band. In other words, one can circulate an arbitrary charge in the loop formed by the junction and the resistance, without changing the properties of the system's ground state.

## 3. In the RSJ, “the” ground state has no definite symmetry with respect to the phase.

The material in this Appendix shows that the infinite ground state degeneracy of the RSJ makes it pointless to debate about what ought to be “the” symmetry of “the” ground state with respect to the junction phase. This should settle the longstanding debate on whether a galvanically-connected non-superconducting environment forces

one to consider the JJ phase as an “extended” variable (as opposed to “compact” in the CPB). As explained above, the junction phase in the RSJ is not measurable; there is no actual physical meaning associated to the localized or delocalized symmetry of a given state in the phase representation, and, correspondingly, no measurement can assess whether it is localized or delocalized, extended or compact. It can also be regarded as the reason why Schmid’s prediction of a localization|delocalization transition was erroneous: in this system, it does not make much sense. The translation invariance and the ensuing multiplicity of the ground states in the RSJ clearly differentiate this system from the akin spin-boson problem regarding the possibility of a spontaneous symmetry breaking caused by dissipation.

#### 4. Recovery of the CPB physics in the $R \rightarrow \infty$ limit

The CPB has a quasicharge ground band with a finite depth  $E_S > 0$  (the so-called phase slip energy) and a 2e-periodicity which reflects the charge quantization on the island of the device. At a non-integer quasicharge  $q$  on this band, there is a finite constant charge on the capacitor (and there is a voltage across it). In this state of the device, if we now connect a resistor across the junction, the resistor drains away the charge on the capacitor and the newly made RSJ eventually reaches its flat-band ground state at times scales longer than  $RC$ . However, in the  $R \rightarrow \infty$  limit this relaxation takes an infinite time and one permanently observes the CPB physics, with a static gate charge.

In other words, static charging effects (often called Coulomb blockade effects) only occur in systems with an island. In the RSJ, a resistor with  $R < \infty$  suppresses the CPB island, making the ground band flat. But even when the circuit no longer has an island, dynamical charging effects may still be observed in it (*e.g.* by driving it non-adiabatically in dc or ac, see E5), similar to dynamical Coulomb blockade in island-less normal-state circuits. Note however that, in spite of having a genuine island, the CPB is dc-superconducting for a small enough current (see II A), even though the curvature of its quasicharge ground band could suggest to regard it as a capacitor.

Could it be that for  $R_Q < R < \infty$ , the symmetries of the Hamiltonian get spontaneously broken, such that the ground state is no longer invariant w.r.t. to charge translation, resulting in a non-flat quasicharge ground band? As just discussed, such non-flat ground band indicates the system has an island, and that would imply that the resistor became insulating, which would contradict the behavior assumed in the first place for the resistor.

#### 5. Stability of the superconducting ground state at finite current bias

In this subsection, we critically examine the superconducting response of the RSJ to a dc current bias, obtained in Sec. IV (Fig. 5) using stochastic Liouville, and discussed in Sec. V. The Hamiltonian of the dc-current-biased RSJ is  $H = H_0 - \varphi_0 I_b \varphi$ . At  $I_b \neq 0$ , the potential of this Hamiltonian is not bounded from below. In that case, the localized states we obtain from our stochastic Liouville method, slightly off-centered from  $\varphi = 0$ , can, at best, only be metastable (just as in the standard tilted washboard image of current-biased JJs). However, in our approach, no runaway to a dissipative state can occur because the states are confined by the counter-term. How confident can we be that this superconducting linear response result we find is not merely an artifact of the method?

By applying a time-dependent unitary transformation  $U(t) = e^{-iI_b \varphi t / 2e}$  to the above current-biased Hamiltonian, we obtain the transformed time-dependent Hamiltonian

$$\tilde{H} = U H U^\dagger + i \hbar \dot{U} U^\dagger = E_C \left( N + \frac{I_b t}{2e} \right)^2 - E_J \cos \varphi + \sum_n 4e^2 \frac{N_n^2}{2C_n} + \varphi_0^2 \frac{(\varphi_n - \varphi)^2}{2L_n}$$

where the potential is bounded as in (1) and where the bias current now appears as a linear-in-time “offset charge” for the CPB. The above Bloch state  $|\Phi_q\rangle$  (E2) with the quasicharge  $q = I_b t / 2e$  is an exact instantaneous (reduced) ground state for  $\tilde{H}$  at time  $t$ . Hence, as long as it can follow adiabatically its flat quasicharge ground band, the system will remain in a zero-voltage state with the junction sustaining the (super)current flow. Such adiabaticity is guaranteed by general theorems [60, 61] at vanishing  $\dot{q}$ , and the superconducting linear response independently worked out in II A confirms that. The linear-response-displaced localized states obtained with our stochastic Liouville method in Fig. 5 correspond to this adiabatic evolution; they are valid metastable solutions, at least at vanishing bias. This confirms that the dc  $I - V$  characteristic of the RSJ at equilibrium is vertical at the origin.

However, when increasing the current bias  $I_b$  (or  $\dot{q}$ ), at some point, adiabatic evolution in the ground band is no longer possible (in any case, one can expect a hard limit at  $|I_b| = I_0$ ); the metastable localized ground state then occasionally experiences phase slips due to macroscopic quantum tunneling through the cosine potential barrier or thermal activation over it, and the junction state gradually or suddenly departs from zero voltage, depending on whether the phase motion is over- or under-damped by the resistance. This physics of the supercurrent branch was broadly understood [44–46] well before Schmid’s work. Caldeira and Leggett completed the understanding of this loss

of adiabaticity by evaluating quantitatively the phase slip rate out of the metastable states for all parameters [1]. They showed that dissipation reduces quantum tunneling of the phase, thereby increasing the lifetime of the metastable state and the ability of the junction to sustain a supercurrent. This is consistent with our conclusion in Sec. V that, at equilibrium, a junction shunted by a resistor is always more superconducting than an unshunted junction.

If one now considers an ac charge drive with a fixed finite amplitude but variable frequency, the above superconducting adiabatic dynamics can only occur at low enough frequency. In that regime, the junction behaves inductively, with an inductance given by the linear response value (7). At sufficiently high frequency adiabaticity is lost, and the behavior is the capacitive response of the CPB ground band at zero offset charge. In-between, one expects a crossover at a given frequency (depending non-linearly on the drive amplitude) with, at that point, likely, the response of the resistor. This explains why uncontrolled noise in experiments may spoil the thermal equilibrium superconducting linear response and the observation of a supercurrent branch at the origin. Similar crossovers from inductive to capacitive can be expected when varying other parameters.

o

- 
- [1] A. O. Caldeira and A. J. Leggett. Quantum tunnelling in a dissipative system. *Annals of Physics*, 149(2):374–456, September 1983. doi:10.1016/0003-4916(83)90202-6.
- [2] John Clarke, Andrew N. Cleland, Michel H. Devoret, Daniel Esteve, and John M. Martinis. Quantum Mechanics of a Macroscopic Variable: The Phase Difference of a Josephson Junction. *Science*, 239(4843):992–997, February 1988. doi:10.1126/science.239.4843.992.
- [3] Albert Schmid. Diffusion and Localization in a Dissipative Quantum System. *Physical Review Letters*, 51(17):1506–1509, October 1983. doi:10.1103/PhysRevLett.51.1506.
- [4] S. A. Bulgadaev. Phase diagram of a dissipative quantum system. *JETP Letters*, 39(6):315–319, 1984.
- [5] Matthew P. A. Fisher and Wilhelm Zwerger. Quantum Brownian motion in a periodic potential. *Physical Review B*, 32(10):6190–6206, November 1985. doi:10.1103/PhysRevB.32.6190.
- [6] F. Guinea, V. Hakim, and A. Muramatsu. Diffusion and Localization of a Particle in a Periodic Potential Coupled to a Dissipative Environment. *Physical Review Letters*, 54(4):263–266, January 1985. doi:10.1103/PhysRevLett.54.263.
- [7] C. Aslangul, N. Pottier, and D. Saint-James. Quantum ohmic dissipation: Particle on a one-dimensional periodic lattice. *Physics Letters A*, 111(4):175–178, September 1985. doi:10.1016/0375-9601(85)90570-5.
- [8] A. D. Zaikin and S. V. Panyukov. Dynamics of a quantum dissipative system: Duality between coordinate and quasimomentum spaces. *Physics Letters A*, 120(6):306–311, March 1987. doi:10.1016/0375-9601(87)90677-3.
- [9] Gerd Schön and A. D. Zaikin. Quantum coherent effects, phase transitions, and the dissipative dynamics of ultra small tunnel junctions. *Physics Reports*, 198(5):237–412, December 1990. doi:10.1016/0370-1573(90)90156-V.
- [10] Gert-Ludwig Ingold and Hermann Grabert. Effect of Zero Point Phase Fluctuations on Josephson Tunneling. *Physical Review Letters*, 83(18):3721–3724, November 1999. doi:10.1103/PhysRevLett.83.3721.
- [11] Carlos P. Herrero and Andrei D. Zaikin. Superconductor-insulator quantum phase transition in a single Josephson junction. *Physical Review B*, 65(10):104516, February 2002. doi:10.1103/PhysRevB.65.104516.
- [12] Naoki Kimura and Takeo Kato. Temperature dependence of zero-bias resistances of a single resistance-shunted Josephson junction. *Physical Review B*, 69(1):012504, January 2004. doi:10.1103/PhysRevB.69.012504.
- [13] Heiner Kohler, Francisco Guinea, and Fernando Sols. Quantum electrodynamic fluctuations of the macroscopic Josephson phase. *Annals of Physics*, 310(1):127–154, March 2004. doi:10.1016/j.aop.2003.08.014.
- [14] Philipp Werner and Matthias Troyer. Efficient Simulation of Resistively Shunted Josephson Junctions. *Physical Review Letters*, 95(6):060201, August 2005. doi:10.1103/PhysRevLett.95.060201.
- [15] Sergei L. Lukyanov and Philipp Werner. Resistively shunted Josephson junctions: Quantum field theory predictions versus Monte Carlo results. *Journal of Statistical Mechanics: Theory and Experiment*, 2007(06):P06002, 2007. doi:10.1088/1742-5468/2007/06/P06002.
- [16] C. L. Kane and Matthew P. A. Fisher. Transport in a one-channel Luttinger liquid. *Physical Review Letters*, 68(8):1220–1223, February 1992. doi:10.1103/PhysRevLett.68.1220.
- [17] Emanuele Dalla Torre and Eran Sela. Viewpoint: Circuit Simulates One-Dimensional Quantum System. *Physics*, 11, September 2018. doi:10.1103/Physics.11.94.
- [18] A. Murani, N. Bourlet, H. le Sueur, F. Portier, C. Altimiras, D. Esteve, H. Grabert, J. Stockburger, J. Ankerhold, and P. Joyez. Absence of a Dissipative Quantum Phase Transition in Josephson Junctions. *Physical Review X*, 10(2):021003, April 2020. doi:10.1103/PhysRevX.10.021003.
- [19] Matthias Vojta. Quantum phase transitions. *Reports on Progress in Physics*, 66(12):2069–2110, November 2003. doi:10.1088/0034-4885/66/12/R01.
- [20] Tom Morel and Christophe Mora. Double-periodic Josephson junctions in a quantum dissipative environment. *Physical Review B*, 104(24):245417, December 2021. doi:10.1103/PhysRevB.104.245417.
- [21] Kanta Masuki, Hiroyuki Sudo, Masaki Oshikawa, and Yuto Ashida. Absence versus Presence of Dissipative Quantum Phase Transition in Josephson Junctions. *Physical Review Letters*, 129(8):087001, August 2022. doi:10.1103/PhysRevLett.129.087001.



- [22] Théo Sépulcre, Serge Florens, and Izak Snyman. Comment on "Absence versus Presence of Dissipative Quantum Phase Transition in Josephson Junctions", October 2022. [arXiv:2210.00742](https://arxiv.org/abs/2210.00742), [doi:10.48550/arXiv.2210.00742](https://doi.org/10.48550/arXiv.2210.00742).
- [23] Manuel Houzet, Tsuyoshi Yamamoto, and Leonid I. Glazman. Microwave spectroscopy of Schmid transition, August 2023. [arXiv:2308.16072](https://arxiv.org/abs/2308.16072), [doi:10.48550/arXiv.2308.16072](https://doi.org/10.48550/arXiv.2308.16072).
- [24] Roman Kuzmin, Nitish Mehta, Nicholas Grabon, Raymond A. Mencia, Amir Burshtein, Moshe Goldstein, and Vladimir E. Manucharyan. Observation of the Schmid-Bulgadaev dissipative quantum phase transition, April 2023. [arXiv:2304.05806](https://arxiv.org/abs/2304.05806), [doi:10.48550/arXiv.2304.05806](https://doi.org/10.48550/arXiv.2304.05806).
- [25] Romain Daviet and Nicolas Dupuis. Nature of the Schmid transition in a resistively shunted Josephson junction. *Physical Review B*, 108(18):184514, November 2023. [doi:10.1103/PhysRevB.108.184514](https://doi.org/10.1103/PhysRevB.108.184514).
- [26] Luca Giacomelli and Cristiano Ciuti. Emergent quantum phase transition of a Josephson junction coupled to a high-impedance multimode resonator, July 2023. [arXiv:2307.06383](https://arxiv.org/abs/2307.06383), [doi:10.48550/arXiv.2307.06383](https://doi.org/10.48550/arXiv.2307.06383).
- [27] Nicolas Paris, Luca Giacomelli, Romain Daviet, Cristiano Ciuti, Nicolas Dupuis, and Christophe Mora. Resilience of the quantum critical line in the Schmid transition, July 2024. [arXiv:2407.01699](https://arxiv.org/abs/2407.01699), [doi:10.48550/arXiv.2407.01699](https://doi.org/10.48550/arXiv.2407.01699).
- [28] Ryogo Kubo. Statistical-Mechanical Theory of Irreversible Processes. I. General Theory and Simple Applications to Magnetic and Conduction Problems. *Journal of the Physical Society of Japan*, 12(6):570–586, June 1957. [doi:10.1143/JPSJ.12.570](https://doi.org/10.1143/JPSJ.12.570).
- [29] Vladimir E. Manucharyan, Jens Koch, Leonid I. Glazman, and Michel H. Devoret. Fluxonium: Single Cooper-Pair Circuit Free of Charge Offsets. *Science*, 326(5949):113–116, October 2009. [doi:10.1126/science.1175552](https://doi.org/10.1126/science.1175552).
- [30] Jens Koch, V. Manucharyan, M. H. Devoret, and L. I. Glazman. Charging Effects in the Inductively Shunted Josephson Junction. *Physical Review Letters*, 103(21):217004, November 2009. [doi:10.1103/PhysRevLett.103.217004](https://doi.org/10.1103/PhysRevLett.103.217004).
- [31] R. P. Feynman and F. L. Vernon. The theory of a general quantum system interacting with a linear dissipative system. *Annals of Physics*, 24:118–173, October 1963. [doi:10.1016/0003-4916\(63\)90068-X](https://doi.org/10.1016/0003-4916(63)90068-X).
- [32] Hermann Grabert, Peter Schramm, and Gert-Ludwig Ingold. Quantum Brownian motion: The functional integral approach. *Physics Reports*, 168(3):115–207, October 1988. [doi:10.1016/0370-1573\(88\)90023-3](https://doi.org/10.1016/0370-1573(88)90023-3).
- [33] Ulrich Weiss. *Quantum Dissipative Systems*. WORLD SCIENTIFIC, 4th edition, 2012. [doi:10.1142/8334](https://doi.org/10.1142/8334).
- [34] J. Hubbard. Calculation of partition functions. *Physical Review Letters*, 3(2):77–78, July 1959. [doi:10.1103/PhysRevLett.3.77](https://doi.org/10.1103/PhysRevLett.3.77).
- [35] R. L. Stratonovich. On a method of calculating quantum distribution functions. *Soviet Physics Doklady*, 2:416, July 1957.
- [36] Jürgen T. Stockburger and Hermann Grabert. Exact c-Number Representation of Non-Markovian Quantum Dissipation. *Physical Review Letters*, 88(17):170407, April 2002. [doi:10.1103/PhysRevLett.88.170407](https://doi.org/10.1103/PhysRevLett.88.170407).
- [37] Jeremy M. Moix, Yang Zhao, and Jianshu Cao. Equilibrium-reduced density matrix formulation: Influence of noise, disorder, and temperature on localization in excitonic systems. *Physical Review B*, 85(11):115412, March 2012. [doi:10.1103/PhysRevB.85.115412](https://doi.org/10.1103/PhysRevB.85.115412).
- [38] G. M. G. McCaul, C. D. Lorenz, and L. Kantorovich. Partition-free approach to open quantum systems in harmonic environments: An exact stochastic Liouville equation. *Physical Review B*, 95(12):125124, March 2017. [doi:10.1103/PhysRevB.95.125124](https://doi.org/10.1103/PhysRevB.95.125124).
- [39] Michael Riesch and Christian Jirauschek. Analyzing the positivity preservation of numerical methods for the Liouville-von Neumann equation. *Journal of Computational Physics*, 390:290–296, August 2019. [doi:10.1016/j.jcp.2019.04.006](https://doi.org/10.1016/j.jcp.2019.04.006).
- [40] Hermann Grabert, Ulrich Weiss, and Peter Talkner. Quantum theory of the damped harmonic oscillator. *Zeitschrift für Physik B Condensed Matter*, 55(1):87–94, March 1984. [doi:10.1007/BF01307505](https://doi.org/10.1007/BF01307505).
- [41] A. Grimm, F. Blanchet, R. Albert, J. Leppäkangas, S. Jebari, D. Hazra, F. Gustavo, J.-L. Thomassin, E. Dupont-Ferrier, F. Portier, and M. Hofheinz. Bright On-Demand Source of Antibunched Microwave Photons Based on Inelastic Cooper Pair Tunneling. *Physical Review X*, 9(2):021016, April 2019. [doi:10.1103/PhysRevX.9.021016](https://doi.org/10.1103/PhysRevX.9.021016).
- [42] Philippe Joyez. Self-Consistent Dynamics of a Josephson Junction in the Presence of an Arbitrary Environment. *Physical Review Letters*, 110(21):217003, May 2013. [doi:10.1103/PhysRevLett.110.217003](https://doi.org/10.1103/PhysRevLett.110.217003).
- [43] This Gaussian result (where the  $2\pi$  translation invariance of the phase is lost) suggests that the effective Josephson coupling can be strongly suppressed by phase fluctuations occurring across large impedances. Our present exact results show that, actually, the effective Josephson coupling  $E_J(\cos\varphi)$  has the lower bound  $E_J^2/E_C$ .
- [44] Yu. M. Ivanchenko and L. A. Zil'berman. The Josephson Effect in Small Tunnel Contacts. *Soviet Journal of Experimental and Theoretical Physics*, 28:1272, June 1969.
- [45] D. E. McCumber. Effect of ac Impedance on dc Voltage-Current Characteristics of Superconductor Weak-Link Junctions. *Journal of Applied Physics*, 39:3113–3118, June 1968. [doi:10.1063/1.1656743](https://doi.org/10.1063/1.1656743).
- [46] W. C. Stewart. Current-Voltage Characteristics of Josephson Junctions. *Applied Physics Letters*, 12:277–280, April 1968. [doi:10.1063/1.1651991](https://doi.org/10.1063/1.1651991).
- [47] Audrey Cottet. *Implémentation d'un bit quantique dans un circuit supraconducteur / Implementation of a quantum bit in a superconductor*. PhD thesis, Université Pierre et Marie Curie - Paris VI, September 2002.
- [48] Jens Koch, Terri M. Yu, Jay Gambetta, A. A. Houck, D. I. Schuster, J. Majer, Alexandre Blais, M. H. Devoret, S. M. Girvin, and R. J. Schoelkopf. Charge insensitive qubit design derived from the Cooper pair box. *Physical Review A*, 76(4):042319, October 2007. [arXiv:cond-mat/0703002](https://arxiv.org/abs/cond-mat/0703002), [doi:10.1103/PhysRevA.76.042319](https://doi.org/10.1103/PhysRevA.76.042319).
- [49] NIST digital library of mathematical functions: §28.12 Mathieu Functions of Noninteger Order. <https://dlmf.nist.gov/28.12>.
- [50] Philipp Werner and Matthias Troyer. A cluster algorithm for resistively shunted Josephson junctions, August 200. [arXiv:cond-mat/0409664](https://arxiv.org/abs/cond-mat/0409664), [doi:10.48550/arXiv.cond-mat/0409664](https://doi.org/10.48550/arXiv.cond-mat/0409664).
- [51] S. Jezouin, M. Albert, F. D. Parmentier, A. Anthore, U. Gennser, A. Cavanna, I. Safi, and F. Pierre. Tomonaga-Luttinger

- physics in electronic quantum circuits. *Nature Communications*, 4(1):1802, April 2013. doi:10.1038/ncomms2810.
- [52] F. D. Parmentier, A. Anthore, S. Jezouin, H. le Sueur, U. Gennser, A. Cavanna, D. Mailly, and F. Pierre. Strong back-action of a linear circuit on a single electronic quantum channel. *Nature Physics*, 7(12):935–938, December 2011. doi:10.1038/nphys2092.
- [53] A. Anthore, Z. Iftikhar, E. Boulat, F. D. Parmentier, A. Cavanna, A. Ouerghi, U. Gennser, and F. Pierre. Circuit Quantum Simulation of a Tomonaga-Luttinger Liquid with an Impurity. *Physical Review X*, 8(3):031075, September 2018. doi:10.1103/PhysRevX.8.031075.
- [54] Jan von Delft and Herbert Schoeller. Bosonization for beginners — refermionization for experts. *Annalen der Physik*, 510(4):225–305, 1998. doi:10.1002/andp.19985100401.
- [55] H. J. Schulz, G. Cuniberti, and P. Pieri. Fermi Liquids and Luttinger Liquids. In G. Morandi, P. Sodano, A. Tagliacozzo, and V. Tognetti, editors, *Field Theories for Low-Dimensional Condensed Matter Systems: Spin Systems and Strongly Correlated Electrons*, pages 9–81. Springer, Berlin, Heidelberg, 2000. doi:10.1007/978-3-662-04273-1\_2.
- [56] Vinay Ambegaokar and Alexis Baratoff. Tunneling Between Superconductors. *Physical Review Letters*, 10(11):486–489, June 1963. doi:10.1103/PhysRevLett.10.486.
- [57] A. Murani, N. Bourlet, H. le Sueur, F. Portier, C. Altimiras, D. Esteve, H. Grabert, J. Stockburger, J. Ankerhold, and P. Joyez. Reply to “Comment on ‘Absence of a Dissipative Quantum Phase Transition in Josephson Junctions’”. *Physical Review X*, 11(1):018002, March 2021. doi:10.1103/PhysRevX.11.018002.
- [58] D. Loss and K. Mullen. Effect of dissipation on phase periodicity and the quantum dynamics of Josephson junctions. *Physical Review A*, 43(5):2129–2138, March 1991. doi:10.1103/PhysRevA.43.2129.
- [59] Kieran Mullen, Daniel Loss, and H. T. C. Stoof. Resonant phenomena in compact and extended systems. *Physical Review B*, 47(5):2689–2706, February 1993. doi:10.1103/PhysRevB.47.2689.
- [60] Joseph E. Avron and Alexander Elgart. Adiabatic Theorem without a Gap Condition. *Communications in Mathematical Physics*, 203:445–463, June 1999. doi:10.1007/s002200050620.
- [61] Daniel Burgarth, Paolo Facchi, Giovanni Gramegna, and Kazuya Yuasa. One bound to rule them all: From Adiabatic to Zeno. *Quantum*, 6:737, June 2022. doi:10.22331/q-2022-06-14-737.